Theme D

Evaluation of Consequences of Collisions
Evaluation des conséquences de collisions
Beurteilung der Folgen von Kollisionen

Leere Seite

Blank page

Page vide

Evaluation of Ship-Bridge Pier Impact and of Islands as Protection

Chocs de bateaux contre des piles de ponts et îlots protecteurs

Schiffskollisionen mit Brückenpfeilern und Schutzinseln

Vladimir MINORSKY
Form. Princ. Naval Arch. and Dir.
George G. Sharp Inc.
New York, NY, USA

Vladimir Minorsky, born 1916, obtained a degree in Naval Architecture and Marine Engineering frem M.I.T., Cambridge 1939. Worked as Naval Architect 1939-1960 and 1966-1978 with George Sharp Inc. on the design of commercial and naval ships. During 1960-1966 he was Chief Design Engineer with DeLong Corp. of New York, working on the design of offshore platforms, and jack-up barges.

SUMMARY

The paper discusses the background of ship impact studies and provides a simple method to calculate impact forces delivered by ships when hitting relatively immovable objects such as bridge piers. It also offers a few thoughts on the hydrodynamic reasons for such collisions, and gives a method for calculating the ship stopping capability of artificial islands.

RÉSUMÉ

Le rapport rappelle les études de collisions de navires et propose une méthode simple de calcul des forces d'impact de navires en collision avec des objets relativement immobiles, tels que les piles de ponts. Le rapport traite des causes hydrodynamiques de ces collisions et donne une methode de calcul de la capacité à arrêter les navires qu'ont les îlots protecteurs.

ZUSAMMENFASSUNG

Der Bericht erörtert den Hintergrund der Untersuchungen im Bereich der verschiedenen Auswirkungen von Schiffen und stellt eine einfache Methode dar zur Berechnung der Auswirkungen der Schiffe, wenn sie mit verhältnismässig immobilen Gegenständen, wie z.B. Brückenpfeilern, zusammenstoßen. Dieser Bericht schließt ebenfalls einige Betrachtungen über die hydrodynamischen Ursachen solcher Kollisionen und eine Methode für die Berechnung der Fähigkeit künstlicher Inseln zur Anhaltung von Schiffen ein.

1. BACKGROUND

Before 1959 collisions interested Naval Architects only insofar as they resulted
in explosions or the loss of a vessel. With the advent of nuclear propulsion,
designers were faced with the possibility that the reactor could be broached in
a collision. Other than the Russian icebreakers operating in the Arctic Ocean
where the chances of a collision were almost nil, "Savannah" was the first non
military nuclear vessel. It was designed to carry cargo and passengers world-
wide. The question which had to be answered at the time was: "What is the size
and speed of a vessel which can broach its reactor in a collision?".

In the US Maritime Administration's Safety Assessment for "Savannah" a semi-
empirical solution was used which gave a relationship between energy absorbed in
a collision and the volume of selected steel members destroyed [1]. The basis
for the method was collision data compiled by the US Coast Guard. This concept
was also used in the reactor protection calculations of "Otto Hahn" and "Mutsu".
At the time of "Mutsu's" design a large amount of original work in the field of
collision research was done in Japan by a team of distinguished scientists and
engineers [2]. In the late 60's personnel of GKSS in West Germany ran collision
tests on models of the "Otto Hahn" [3] and in the 1970's they developed the
rationale for a structural protective grid made of webs and stringers spaced
about 1 m apart at the side shell abreast of the reactor compartment. The grid
was designed to stop virtually any striking vessel. This idea was also consid-
ered for "Savannah", but not incorporated for economic reasons; also, at the
time, experiments could not be scheduled to verify the scheme.

In connection with their collision research GKSS tested a series of bow models
built to scales of 1/7.5 and 1/12. These bow models, placed on a cart, ran down
a ramp to meet the collision barrier at 90°. This experimental work is described
in a number of papers [4] [5]. In these tests the collision barrier constituted
an almost immovable obstacle, very much like a bridge pier.

About 1975, GKSS and the US Maritime Administration started upon a joint program
of research where some of the tasks allocated to the US Maritime Administration
included statistics on ship accidents and collision probability studies [7], as
well as calculations of impact forces using, to some extent, formulae collected
from various sources by Professor K.A. Reckling [6]. The object of these impact
force calculations was to verify forces measured by GKSS on the model of the
bulbous bow tanker "Esso Malaysia".

This particular research task ran into difficulties on both sides of the Atlantic:
the GKSS established the penetration (bow destruction) for a known kinetic
energy input which was accomplished in two separate, but additive, steps. Un-
fortunately, faulty instrumentation did not provide reliable impact force mea-
surements; as for the calculation of these forces by a "bits and pieces" ap-
proach for successive bow sections, it also encountered problems.

The forces resulting from impact upon certain portions of the bow such as the
centerline bulkhead, the decks and flats, and the hemisphere at the tip of the
bulb, could be calculated with some confidence; however, no satisfactory for-
mulae were available with which to calculate the contributions of the stiffened
side shell plating and stringers which were inclined at an angle to the direc-
tion of impact, or for the curved portions of shell plating which form the
transition from bulb to hull proper. In addition to these uncertainties, this
method of calculation is laborious and time-consuming.

While engaged in an attempt to calculate these impact forces at successive
points, the writer became acquainted with a semi-empirical method for cal-
culating the crippling strength of multicorner (more than two corners) air frame
sections. The method is simple and quick: it appears that it can be applied to
the sections of a ship's bow to give answers sufficiently accurate to satisfy
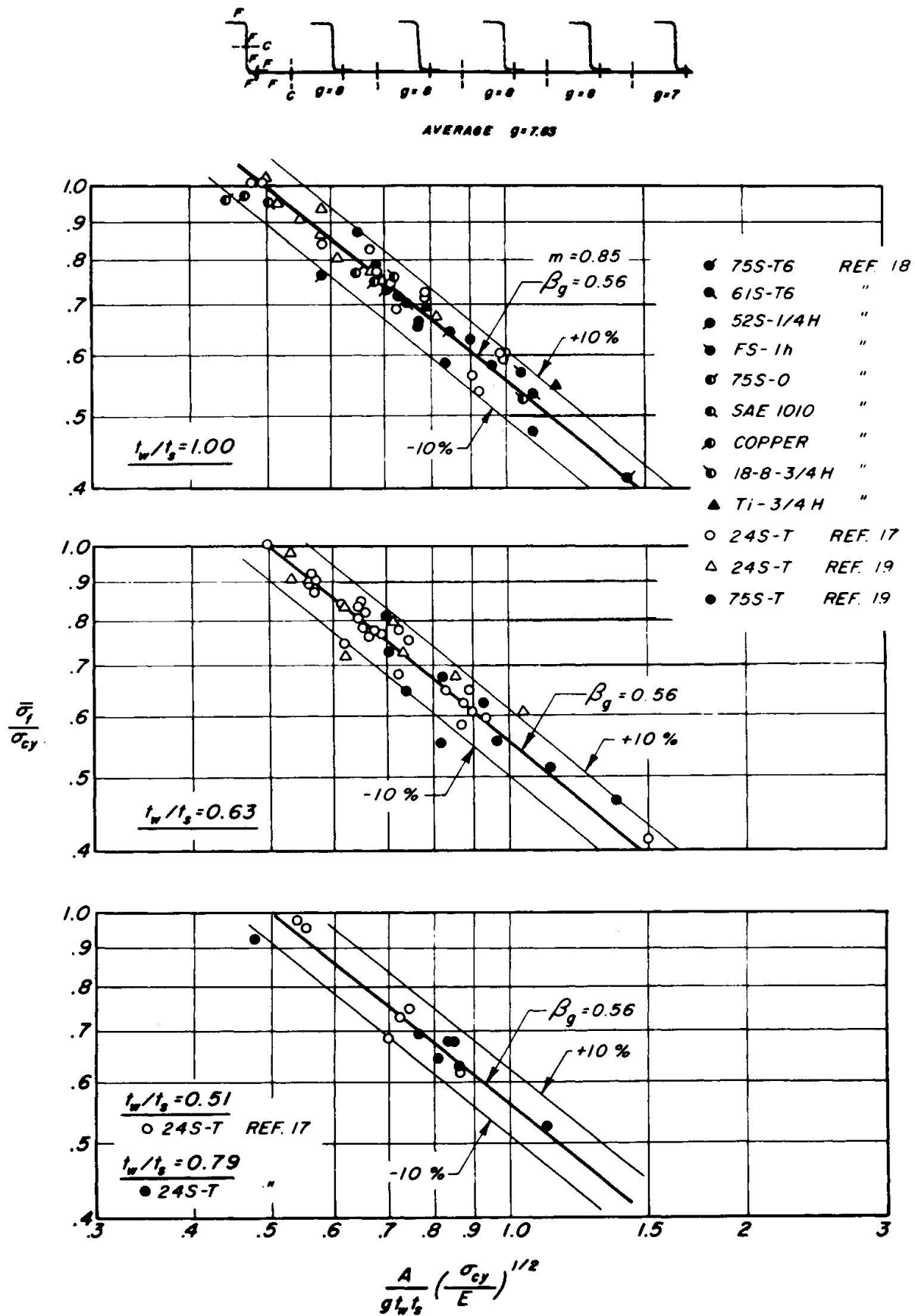
Fig. 1. Crippling data on Z-stiffened panels.
(From ref. [8]).

designers interested in knowing impact forces against bridge piers. The method in question is described by Gerard in [8].

2. GERARD'S SEMI-EMPIRICAL METHOD

Gerard's method is based on many tests performed on stiffened plating using various types of stiffeners and many different materials including a number of aluminium alloys, steel, copper and titanium. Crippling strength is defined as the stress at which secondary instability occurs for thin wall compression members, in the form of a local failure in buckling which exceeds the elastic buckling load. The paper claims accuracy within ± 10%.

Gerard's relationship is defined by the curve of Fig. 1 taken from [8]. The basic equation is:

$$\sigma_F/\sigma_{cy} = 0.56 \left[(\frac{g t_w t_s}{A})(\frac{E}{\sigma_{cy}})^{1/2} \right]^{0.85}$$

where:

σ_F = the crippling strength (Kgf/cm^2),

σ_{cy} = compression yield (Kgf/cm^2),

g = number of cuts plus flanges,

t_w = thickness of stiffening members (cm),

t_s = thickness of skin (cm),

A = area of element (cm^2) and

E = modulus of elasticity (Kgf/cm^2).

Where there are variations in t_w and t_s within a section, a weighting factor can be introduced. In the simple sections considered by Gerard it was thought that an average value for t_w and t_s would be sufficiently accurate. In the case of the "Esso Malaysia" model which has been analysed using Gerard's method, all interior members have a thickness of 1 mm; the value of t_s used is that of most of the shell thickness at a given section; however, the area A of a section takes into account variations in shell thickness. At first impression, the 'g' value used by Gerard seems to be a non-rational and even arbitrary quantity, but upon closer examination, one perceives that it is at the heart of Gerard's method and is an original intuitive contribution.

Examples of 'g' values for different sections are given in Fig. 2 taken from Gerard's paper.

DISTORTED UNLOADED EDGES

ANGLE   PLATE   TUBE

BASIC SECTION   I CUT   4 CUTS
g = 2   2 FLANGES   8 FLANGES
                 3 = g   12 = g

STRAIGHT UNLOADED EDGES

T-SECTION   CRUCIFORM   H-SECTION

BASIC SECTION   0 CUTS   I CUT
g = 3   4 FLANGES   6 FLANGES
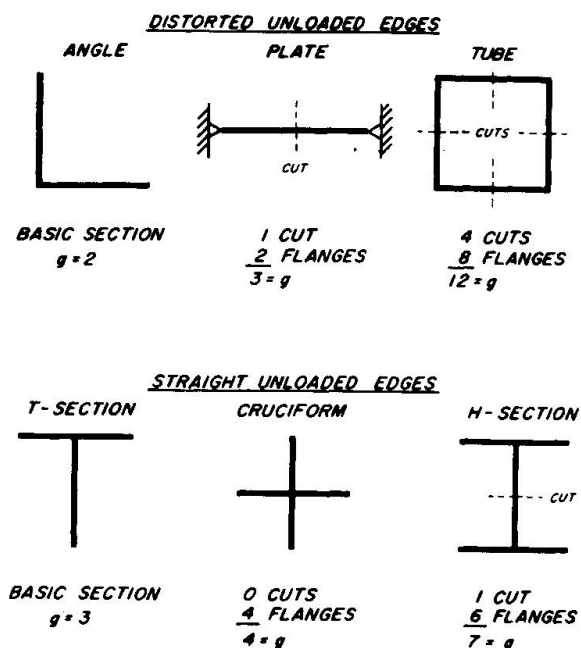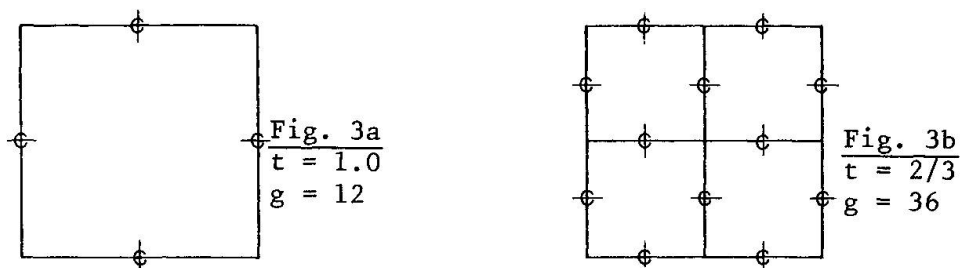   4 = g   7 = g

Fig. 2. Methods of cutting simple elements to determine "g".
(From ref. [8]).

The importance of the 'g' concept is illustrated numerically by Fig. 3a and 3b where ₵ indicates a cut.

Fig. 3a
t = 1.0
g = 12

Fig. 3b
t = 2/3
g = 36

Figures 3a and 3b have the same outside dimensions. Cuts are made so as to produce simple flanged elements. The total cross sectional area A is the same for 3a and 3b when t = 1 in Fig. 3a and t = 2/3 in Fig. 3b. The application of Gerard's relationship shows that 3b has a crippling strength and a resistance to failure 27.6% greater than 3a; conversely, for the same crippling strength, 3b will be lighter than 3a.

3. RESULTS FOR "ESSO MALAYSIA" MODEL

The "Esso Malaysia" is a bulbous bow crude oil carrier built in 1967 by Howaldts-werke-Deutsche Werft. Its characteristics are LOA = 323.7 m, Beam = 47.2 m, Depth = 23.7 m and deadweight 195,000 tonnes. GKSS conducted collision tests (Test 12) on a welded model of its bow to a scale of 1/12.

The crushing of the bow was obtained in two separate blows: first, the model bow was raised 2.16 m to give a first impact energy of 39,100 Kgfm (383 kNm) which resulted in a penetration of 0.50 m; in a second impact the bow was released from a height of 5.35 m, adding 96,800 Kgfm (950 kNm) to the first impact energy for a total of 135,900 Kgfm (1333 kNm). The final penetration was 1.41 m. The model frame spacing is 5.083 cm.

The result of applying Gerard's formula to the model structure is shown in Fig. 4 which plots calculated impact forces in Kgf against frame spacing for the "Esso Malaysia" model.

In Fig. 4 the plot of impact forces OABCDE shows two discontinuities: at frame 158, where the bulb shell plating thickness drops from 0.275 cm to 0.20 cm, and at frame 147, where most of the shell plating thickness drops from 0.20 cm to 0.15 cm (Fig. A-2 in Appendix). Detail calculations are given for these two points in the Appendix.

Values for intermediate points are also given in the Appendix, as well as values which would be obtained if the shell were 0.20 cm thick throughout the bow. This would result in the curve OBCF in Fig. 4.

Returning to curve OABCDE, the average impact force for the range of first impact (0.50m penetration) is 69,000 Kgf (677 kN). The area under this part of the curve is 34,500 Kgfm representing work, as compared to 39,100 Kgfm of energy input, giving an error of 11.7%. The average impact value for the entire curve (1.41 m penetration) is 99,000 Kgfm (971 kNm); the area under the curve is 139,600 Kgfm (1370 kNm), representing work, as compared to 135,900 Kgfm (1333 kNm) of energy input, giving an error of 2.7%.

The maximum impact from calculations in the first phase is 81,900 Kgf (803 kN), and for the entire curve it is 151,000 Kgf (1481 kN). Unfortunately, there is no valid experimental data to compare with these calculated values. It is hoped that in the future satisfactory instrumentation will be available to verify the validity of Gerard's method for maximum impacts as well as for the work done by impact forces.
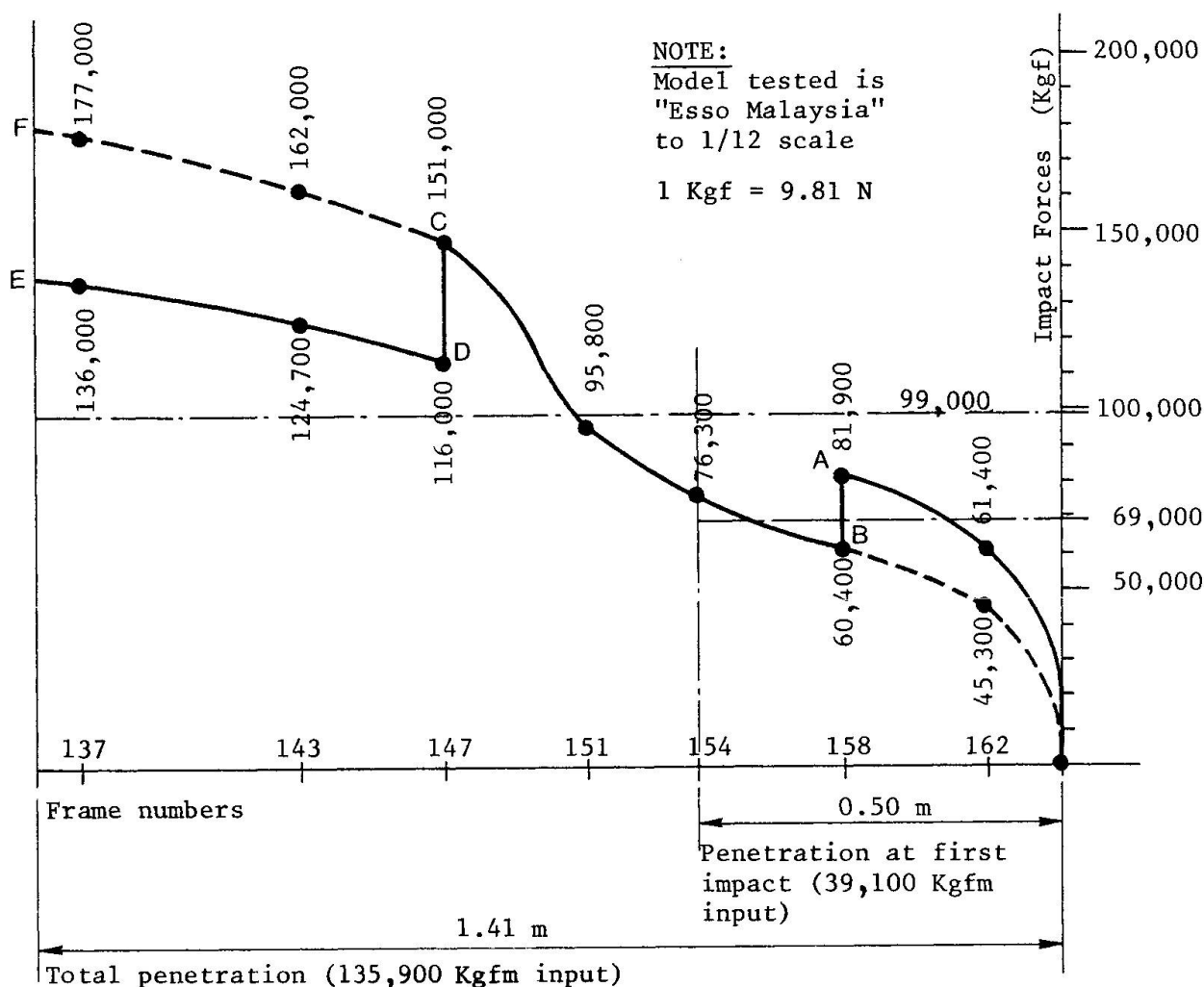
Fig. 4. GKSS model test penetrations versus impact forces from Gerard's method.

In comparing the calcutated energy with that known to have been spent in the testa, Gerard's method gives satisfactory results. It should be mentioned that the collision barrier in the tests was lower than "Esso Malaysia's" main deck. If the deck had been involved, the impact forces would have been higher.

Of particular interest to bridge designers is the full scale impact force: since forces are proportional to the square of scale ratio, the caximum full scale imapct would have been in theory, 12^2 x 151.0 tonnes or 21,700 tonnes. In actuality, one may expect the full scale impact force to be less than that derived from model tests. Scale effect is discussed in [5] for energy. The comments in [5] will also apply to forces: metal grain size is not to scale in the model, which is also subject to excessive strain hardening.

If properly instrumented tests should verify force calculations by Gerard's method, it will be possible to calculate impact directly from scantling drawings of a full size ship and thus eliminate the problems of scale effect.

It is interesting to note that in Fig. 4 the impact value at point A, 81,900 Kgf (803 kN), at frame 158 could be obtained at a penetration of only 0.30 m and an energy of only 20,700 Kgfm (203 kNm), so that a significant impact force can be obtained at a low energy. In studying various ship types which can hit a bridge pier it is important to singel out vessels with hard bows.

It should be easy to program Gerard's method for a computer solution, so that, once the bow sections are available, a solution such as that of Fig. 4, can be obtained in very little time.

The effect of the large lightening holes in the centerline bulkhead (Fig. Al of Appendix) was studied: it was found that the stiffening at the edges of ligaments between holes introduced additional 'cuts and flanges' which compensated for the plating removed by the lightening holes.

Before leaving the subject of Gerard's method, the writer would like to mention that airframe methods of analysis were completely unknown to him prior to attempting the "Esso Malaysia" impact calculation. This points out that there is today an unfortunate tendency to produce narrow specialists. There is much to be gained in becoming aware of what is being done in other branches of engineering.

4. REASONS FOR COLLISIONS OF SHIPS WITH BRIDGES

It is puzzling, to say the least, that there should have been a number of cases where ships equipped with the latest navigational equipment and with beams of only 20 to 30 m hit piers where the clear span was 100 m or more. The Store Baelt report [9] states that the principal reasons for such collisions are human error, mechanical failure and weather conditions. Elsewhere in [9] an Australian correspondent lists tidal current in the navigation direction, ships in ballast, and strong winds as being local reasons for collisions.

There is little one can say about human errors such as that of the skipper who fell asleep at the helm. Perhaps there should be a rule requiring two officers to be present in a pilot house when approaching a bridge.

Mechanical failure seems a very remote possibility if one thinks of a steering breakdown happening at the precise moment when a ship comes to a bridge: the critical time preceding a collision is counted in minutes, compared to a sea voyage of several weeks. For any one voyage the probability that a steering failure will happen at the approach to a bridge is perhaps 5×10^{-5} which, of course, must be multiplied by the probability that a steering failure will happen at all in the lifetime of a ship. It is likely that in many cases collisions blamed on steering failure were caused by some of the reasons listed below.

Besides the above reasons there are hydrodynamic explanations for the loss of steerageway which may not always be understood. Only one such reason was mentioned in [9] : the case of tidal current running with the vessel. If the vessel is going slow ahead, or half ahead with a strong following current, the rudder may not respond to the helm because water is not flowing past the rudder at all, or not fast enough to produce lift on the rudder. The same situation will arise if the officer on watch should be so ill-advised as to order power astern with the object of reducing speed when approaching a bridge: with the screw race no longer impinging upon the rudder, the vessel will lose steerageway, as is well known from vessels executing crash stops on trial. Finally, a vessel moving slow ahead at a slight angle into a strong current may find that its hull acts as a hydrofoil, creating a greater turning moment than can be overcome by the rudder, as shown in Fig. 5.
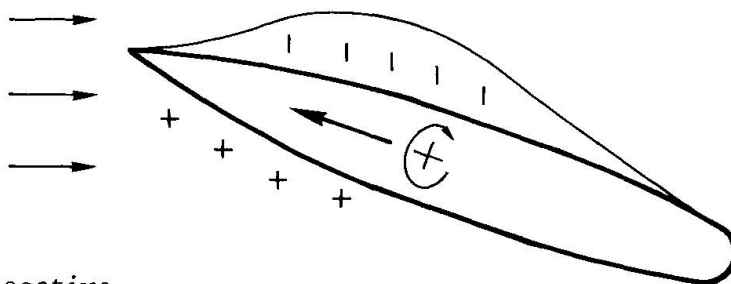

Fig. 5. Turning moment due to negative pressure field caused by current on hull.

The steering problems caused by hydrodynamic conditions, and even those caused by mechanical failure, can be overcome or improved by the use of a bow thruster. This device should be a requirement for any vessel which transits bridges frequently, or is engaged in a trade where it plies busy waterways. At the approach of a bridge the thruster should be activated and rotating at zero blade angle, ready to thrust.

5. THE PROTECTION OF BRIDGE PIERS

5.1 Protective devices

Piers can be protected by fenders on the pier itself, fenders on piles around the pier, clusters of piles, dolphins, or artificial islands.

- Fendering is suitable for protection from barges and small vessels. It cannot stop large vessels.

- Pile clusters (summation of individual piles) or dolphins (a group of piles rigidly tied together at the top) may be too limber in deep water; also, the driving of such piles and their maintenance may be costly. A fairly rigid dolphin of good-sized steel piles may have fair stopping qualities, but it may rupture the side shell of a ship in a glancing encounter: in the case of a tanker this may be disastrous for the environment.

- Artificial islands are without doubt the best and cheapest solution for large vessels. The cheapest material for an island is sand, which can be pumped in situ by dredges. Sand may not be suitable if the location is subject to a breaking surf in stormy weather, or to swift tidal currents; in both instances there may be a scouring action that will carry away part of the island. In such cases coarse gravel or stones (10-15 cm) or cobbles will be preferable. Rip rap of quarried stone or precast elements on an island will stop a vessel very effectively, but it will also rip out the ship's bottom, with consequent damage to the ecology. The writer was consulted for the artificial island protecting the planned nuclear power station for the Atlantic Generating Station. The semi-empirical method used for "Savannah" could be applied to predict the stopping ability of rip rap for an aircraft carrier hitting the island at 32 knots. As the writer recalls it, it was found that the rip rap would have stopped the aircraft carrier in some 35 m, but with considerable damage to the vessel's bottom. The model tests performed for the artificial island in connection with this project were not realistic, because the model island used sand, which could not have been used in that location on account of a heavy surf.

5.2 Calculations of an island's stopping capability

The stopping capability of an island for any vessel can be predicted with good accuracy if the coefficient of friction of the steel bottom sliding up the beach is known. If the vessel's forefoot slides, the coefficient of friction on gravel is 0.40. In the case where the beach of the island is steep, the forefoot may plow it up, with a resulting higher value for the coefficient of friction, the value of which will have to be determined. It should be noted that a vessel in ballast may trim by the stern as much as 2°, which will reduce the angle between keel and beach. The assumption that the forefoot slides up the beach instead of digging into it will always be on the safe side.

In Fig. 6 a wessel is shown first contacting an artificial island at point 0_1, travelling up the beach a distance d, and stopping with the forefoot at the point 0_2.
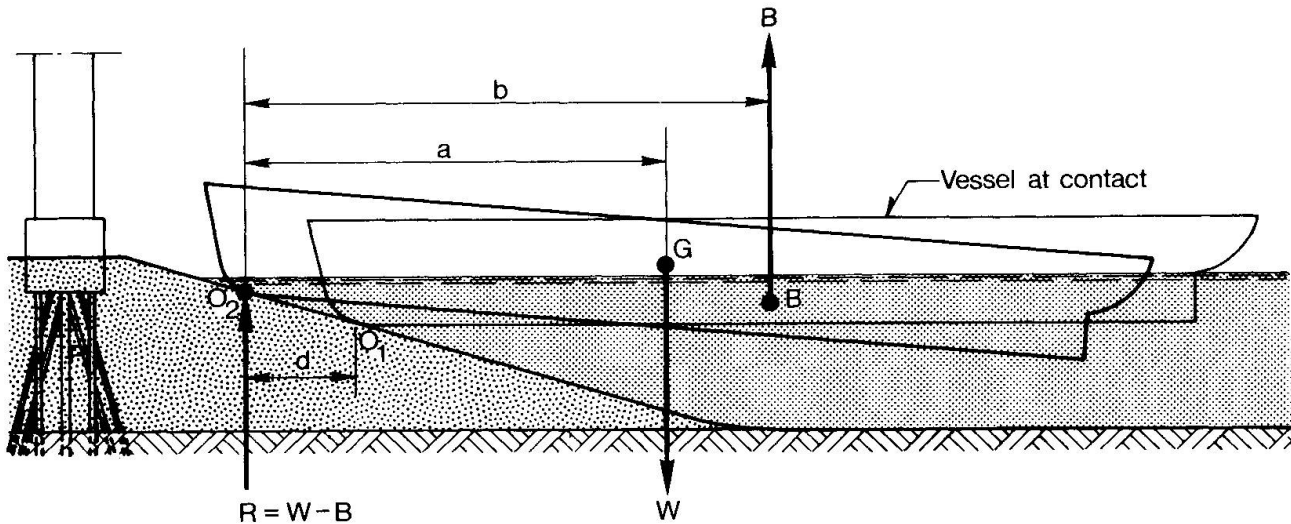
Fig. 6. Weight-buoyancy equations for ship meeting artificial island.

0 being any point along d between O_1 and O_2 and calling:
    W - the ship's displacement,
    B - its buoyancy,
    a - the distance from center of gravity to point 0 and
    b - the distance from center of buoyancy to 0.

The reaction R at point 0 is: $R = W - B$ (1)
For equilibrium, moments about 0 are: $Wa = Bb$ (2)
hence, $R = W(1 - a/b)$

The angle of the ships keel with the horizontal during the travel of the forefoot
up the beach is unknown: if several trim lines are drawn when forefoot is at
point 0, the corresponding ship buoyancy B and longitudinal center of buoyancy b
can be determined for these trim lines using Bonjean curves. Plotting the pro-
duct Bb against the trim line angles, the trim angle for which equation (2) is
satisfied can be established, and knowing B, the reaction R at point 0 is
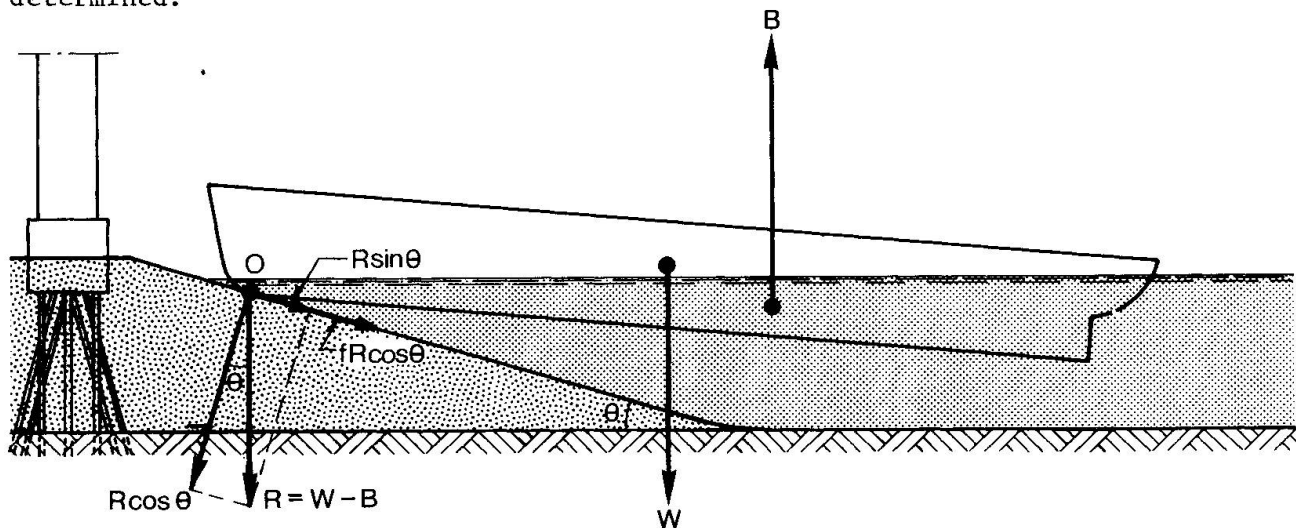determined.

Fig. 7. Forces on ship forefoot.

In Fig. 7 the down slope component of R is $R \sin \theta$. The component normal to the
beach is $R \cos \theta$. In sliding up the beach the forefoot has to overcome a force:
$$F = R \sin \theta + fR \cos \theta$$ (3)
where f is the frictional coefficient.
If $f = 0.40$ and $\theta = 20°$, then $F = 0.718R = 0.718W(1 - a/b)$ (4)
If F is plotted against distance travelled by the forefoot, the area under such

curve is work. The stopping point is where the area equals the kinetic energy of the vessel at contact. As a sample calculation, if a vessel of displacement W = 100,000 tonnes travelling at 7.5 m/sec coasts into an island, its kinetic energy is 286.6 x 10^6 Kgfm (2810 MNm). Assuming that the curve described above is drawn, and that the average force F = 0.10W, the distance to stop is 286.6 x 10^6 Kgfm divided by 10 x 10^6 Kgf = 28.6 m.
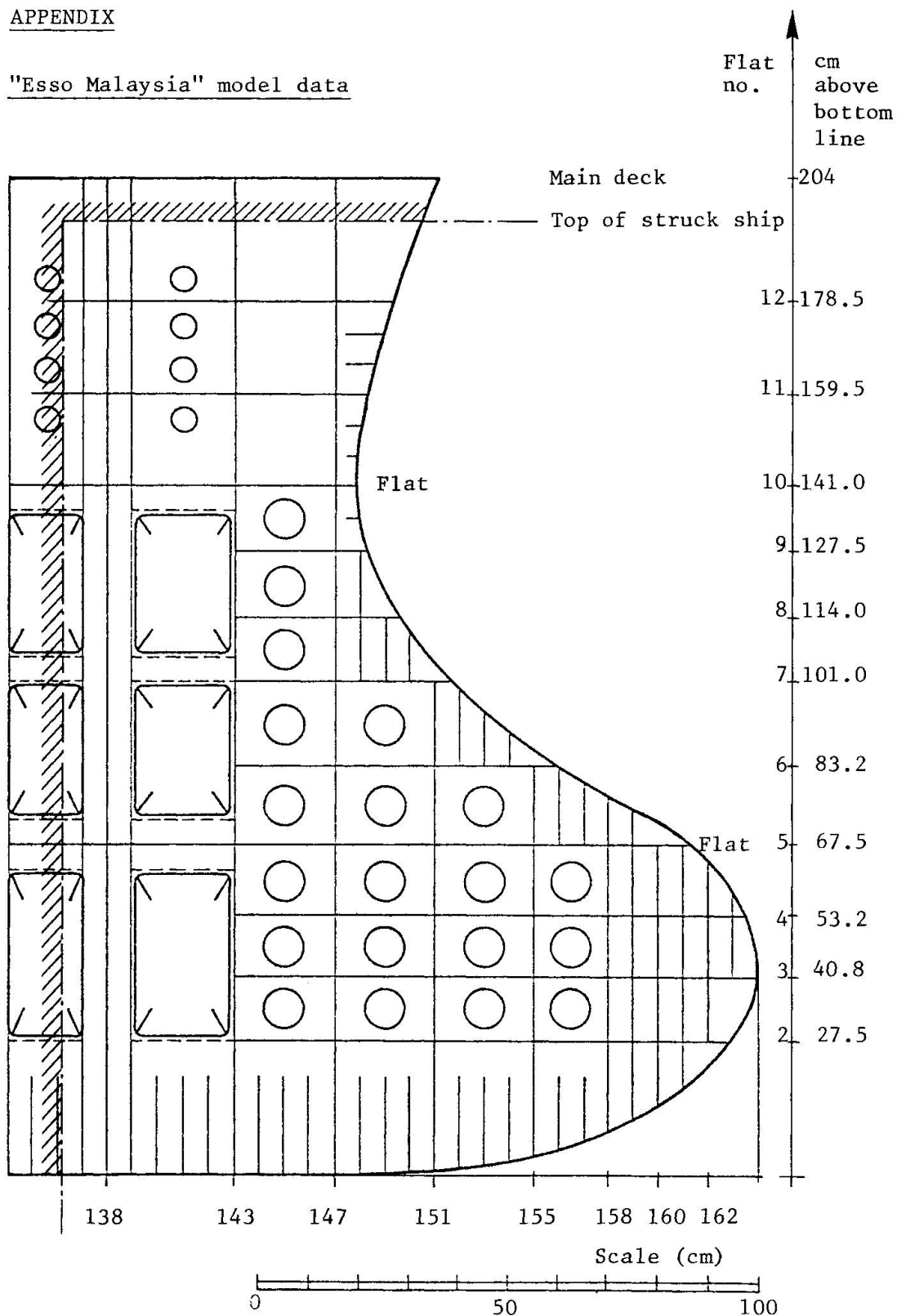
5.3 Tests
While model tests on artificial islands are of great interest, the writer would like to be reassured concerning scale effects, especially for the coefficient of friction. In this connection, it should be fairly simple to run non-destructive tests on a full size ship instrumented to give the required information. It would then be possible to verify the accuracy of model tests by comparing them to full size results.

REFERENCES

1. MINORSKY V., An Analysis of Ship Collisions with Reference to Protection of Nuclear Power Plants. Journal of Ship Research, Oct. 1959.

2. AKITA Y. et al, Studies on Collision Protective Structures of Nuclear Powered Ships. Report 71. The Shipbuilding Research Association of Japan, Tokyo, Japan 1964.

3. WOISIN G., Kollisionsversuche mit Schiffsteilmodellen. Kerntechnik 9, 1967.

4. WOISIN G., Die Kollisionversuche der GKSS. Jahrbuch der Schiffbautechnischen Gesellschaft 1976.

5. WOISIN G., Design against Collisions. International Symposium on Advances in Marine Engineering, Trondheim, Norway, June 1979.

6. RECKLING K. A., Contributions of Elasto and Plastomechanics to Research with Ship Collisions. STG, Berlin, Nov. 1976.

7. MINORSKY V., et al, Ship Accident Studies, Symposium on Safety of Nuclear Ships, Hamburg, December 1977.

8. GERARD G., The Crippling Strength of Compression Elements. Journal of Aero nautical Sciences, January 1958.

9. MINISTERIET FOR OFFENTLIGE ARBEJDER, Investigation into the Ship Collision Problem. The Great Belt Bridge, Copenhagen, Feb. 1979.

APPENDIX
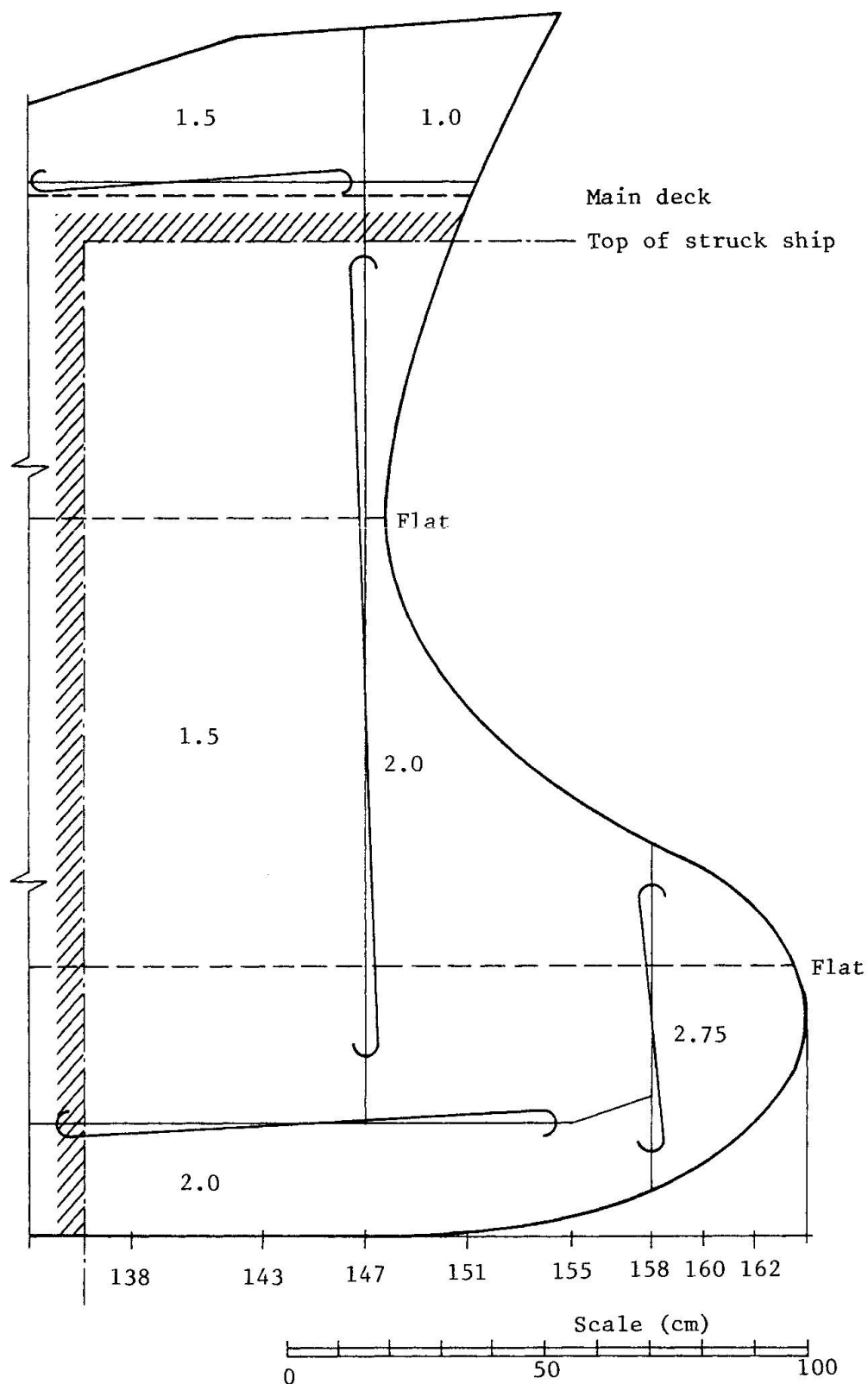
"Esso Malaysia" model data

Fig. A-1   "Esso Malaysia" model. Section at centerline of bulkhead.

NOTE:
All plating: 1mm
Frame spacing 5.09 cm

NOTE:
Frame spacing: 5.09 cm

Fig. A-2   "Esso Malaysia" model. Bow shell plating in mm.

Calculation of crippling forces using Gerard's method.

Frame 157½

g	=	23(cuts) + 46 (flanges) = 69
t_w	=	0.1 cm
t_s	=	0.2 cm
Area	=	64.2 cm^2
σ_{cy}	=	2530 Kgf/cm^2
σ_F/σ_{cy}	=	0.372
σ_F	=	941 Kgf/cm^2
Force	=	60,400 Kgf (592 kN)

Frame 158

g	=	23 (cuts) + 46 (flanges) = 69
t_w	=	0.1 cm
t_s	=	0.275 cm
Area	=	79.0 cm
σ_{cy}	=	2530 Kgf/cm^2
σ_F/σ_{cy}	=	0.4095
σ_F	=	1036 Kgf/cm^2
Force	=	81,900 Kgf (803 kN)

Frame 146½

g	=	55 (cuts) + 121 (flanges) = 176
Area	=	67.4 (shell)
	+	19.0 (bulkhead)
	+	24.6 (flats)
	+	10.4 (stringers)
	+	2.6 (keelson)
		124.0 cm^2

$$\sigma_F/\sigma_{cy} = 0.56\left[\frac{176 \times 0.1 \times 0.15}{124.0} \times 28.8\right]^{0.85}$$

$$= 0.369$$

σ_F = 935 Kgf/cm^2

Force = 116,000 Kgf (1138 kN)

Fig. A-3. Section at frames 157½ - 158.

Scale (cm)

0   50

Fig. A-4. Section at frames 146½ - 147.

Frame 147

g	=	55 (cuts) + 121 (flanges) = 176
Area	=	84.4 (shell)
	+	19.0 (bulkhead)
	+	24.6 (flats)
	+	10.4 (stringers)
	+	2.6 (kellson)

$$141.0 \ cm^2$$

σ_F/σ_{cy}	=	0.423
σ_F	=	1070 Kgf/cm^2
Force	=	151,000 Kgf (1481 kN)

Frame 162

g	=	54
A	=	46.7 cm^2
σ_F	=	1314 Kgf/cm^2
Force	=	61,360 Kgf (602 kN)

With t_s of skin = 20 cm, it would be 45,300 Kgf

Frame 154

g	=	90
A	=	67.2 cm^2
σ_F	=	1136 Kgf/cm^2
Force	=	76,300 Kgf (748 kN)

Frame 151

g	=	112
σ_F	=	1078 Kgf/cm^2
Force	=	95,900 Kgf (940 kN)

Frame 143

g	=	182
A	=	168.8 cm^2
σ_F	=	738 Kgf/cm^2
Force	=	124,700 Kgf (1223 kN)

With t_s of skin = 0.20 cm, it would be 162,000 Kgf (1590 kN)

Frame 137

g   = 205

A   = $152,2 \text{ cm}^2$

σ_F = 844 Kgf/cm^2

Force = $136,000 \text{ Kgf}$ (1334 kN)

With t_s of skin = 0.20 cm, it would be 177,000 Kgf (1736 kN)

Leere Seite
Blank page
Page vide

Modelling of Ship Collisions against Protected Structures
Essais sur modèle de collisions de navires contre des structures de protection
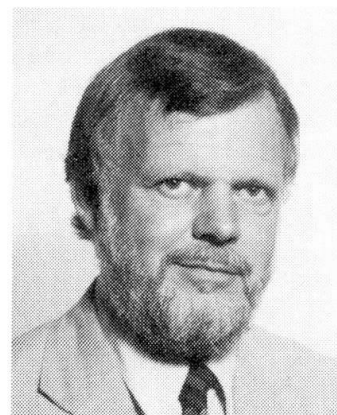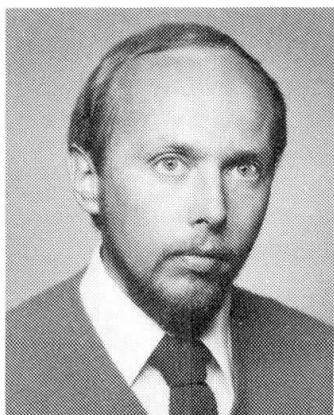## Modellversuche für Schiffkollisionen gegen Schutzbauten

Ole BRINK-KJÆR
Senior Hydraulic Engineer
Danish Hydraulic Institute
Hørsholm, Denmark

Finn Primdahl BRODERSEN
Hydraulic Engineer
Danish Hydraulic Institute
Hørsholm, Denmark

Arne Hasle NIELSEN
Deputy Director
Danish Hydraulic Institute
Hørsholm, Denmark

Ole Brink-Kjær, born 1950, holds M.Sc. and Ph.D. degrees from the Technical University of Denmark. For six years he has been working within computational hydraulics, especially on storm surge and wave modelling. He has been responsible for the assessment of extreme environmental conditions for several offshore and coastal engineering projects.

Finn Primdahl Brodersen, born 1950, got his M.Sc. in civil engineering at the Technical University of Denmark. For 4 years he was working with hydraulic models, mainly concerning breakwater stability and wave disturbance in harbours. Since 1979 he has been involved in the design and supervision of marine pipelines.

Arne Hasle Nielsen, born 1934, holds M.Sc.'s from the Technical University of Denmark (1958), and Berkeley University of California (1962) in Hydraulic and Marine Engineering. After a few years in consulting engineering, he joined DHI in 1964, where he has been in charge of numerous hydraulic studies in many countries.

SUMMARY
This paper describes how model tests and mathematical analysis techniques can be combined to reach a deterministic description of collisions between ships and protective structures, thereby providing an engineering tool which can be applied for the design of protective structures with optimal stopping and deflecting capabilities. Results obtained for the now postponed Great Belt Bridge (Denmark) illustrate the application of this technique for protective rubble mound structures.

RÉSUMÉ
Cet article décrit des essais sur modèle et des techniques d'analyse mathématique pour obtenir une description déterministe de collisions entre des navires et des structures de protection, procurant ainsi un moyen utilisable pour la conception et le projet de structures de protection ayant des capacités optimales d'arrêt et de déviation. Les résultats obtenus pour le "Great Belt Bridge" (Danemark), projet maintenant repoussé à une date ultérieure, illustrent l'application de cette technique aux structures de protection en enrochement.

ZUSAMMENFASSUNG
Dieser Artikel behandelt, wie Modellversuche und mathematische Analysetechnik vereint werden können, um Kollision zwischen Schiff und Schutzbauten zu beschreiben. Hiermit wird ein ingenieurmässiges Werkzeug gegeben, das für den Entwurf von Schutzkonstruktionen, mit optimalen stoppende und abweisenden Eigenschaften, geeignet ist. Resultate von der Grosse-Belt-Brücke, deren Bau jetzt verschoben ist, zeigen die Verwendbarkeit dieser Technik bei Steingeschützten Konstruktionen.

1.   INTRODUCTION

The risks and the consequences of ship collisions are of govering importance for the design of many types of marine structures, such as bridge piers. Optimal design of protective structures requires a general understanding of the deflecting and stopping capabilities of such structures combined with methodologies for the accurate assessment of collision consequences as function of collision circumstances.

Model tests and mathematical analysis techniques can be important tools in the planning and design of protective structures by providing insight in the collision mechanism and the associated impact forces.

The empirical findings on ship collisions as they have been obtained from structural, soil mechanical and hydraulic model tests can be combined with a general mathematical formulation of the collision problem. This allows for a reliable extension of model test results to cover other conditions than those specifically tested. Such techniques were used to study protection islands for the planned Great Belt Bridge (Denmark) and results from these investigations are discussed in the present paper.

This paper describes collisions as function of:

- the speed, course, size, bow shape and hull stiffness of vessel
- the strength and geometrical shape of the protective structure.

The basic equations for the vessel's motion during collisions are presented in Chapter 2. A classical mechanical formulation, which takes into account all six degrees of freedom, is feasible and can be solved with only little computational effort. Basic information on the impact forces arising from the crushing of ship bows is outlined in Chapter 3. The following four chapters 4-7 deal with different combinations of the relative strength of the vessel and the protective structure, i.e. rigid - rigid, deformable - rigid, rigid - deformable and deformable - deformable.

A more detailed description is given in chapter 6 with rigid vessels against deformable protective structures, in this case rubble mound structures. This case is treated in detail because it demonstrates how findings from parallel studies within different engineering areas for a given project can be combined into one deterministic frame and verified against hydraulic model tests. Such tests were carried out for the planning of the now postponed, high level combined road- and railway bridge across the 15 km wide Great Belt (Denmark). Rubble mound structures around the bridge piers appeared to be a promising solution for protecting this bridge against ill-manouvred vessels passing along the main shipping route (20,000 vessels per year) from the North Sea to the Baltic countries. Fully loaded tankers up to 250,000 DWT may navigate in these waters. Existing information on collision between vessels and rubble mound slopes was found to be limited and not useful for design purposes. A series of studies were therefore initiated and interpretated as outlined in Chapter 6.

2.   GENERAL FORMULATION OF EQUATIONS OF MOTION

The equations of the vessel's motion are most conveniently expressed by using two cartesian frames of reference:

1. A fixed cartesian frame of reference, Frame I, with horizontal x- and y-axes and a vertical z-axis.

2. A cartesian frame of reference, Frame A, which is fixed relative to the vessel. For this frame an index $_A$ is used. The origo is placed at the vessel's centre of gravity, and the x_A- and y_A-axis coincide with the vessel's longitudinal and trans-versal axis, respectively.

The translatory displacements of the vessel's centre of gravity are denoted x_G, y_G and z_G.

The angular displacements of the rotational motion around

firstly   -   the vertical axis through the vessel's centre of gravity.
secondly -   the transversal axis of the vessel.
thirdly -   the longitudinal axis of the vessel

are denoted RZ, RY and RX. The sequence of defining these angles is part of the definition. These angular movements are known as yaw, pitch and roll. For small values of the angular displacements, the translatory displacements x_G, y_G and z_G are known as surge, sway and heave.

The relationship between the coordinates of the two frames of reference becomes

$$\begin{bmatrix} x \\ y \\ z \end{bmatrix} = \begin{bmatrix} x_G \\ y_G \\ z_G \end{bmatrix} + \begin{bmatrix} C_{11} & C_{12} & C_{13} \\ C_{21} & C_{22} & C_{23} \\ C_{31} & C_{32} & C_{33} \end{bmatrix} \begin{bmatrix} x_A \\ y_A \\ z_A \end{bmatrix} \quad \text{,where}$$

$C_{11} = \cos RY \cos RZ$
$C_{12} = \sin RX \sin RY \cos RZ - \cos RX \sin RZ$
$C_{13} = \cos RX \sin RY \cos RZ + \sin RX \sin RZ$
$C_{21} = \cos RY \sin RZ$
$C_{22} = \sin RX \sin RY \sin RZ + \cos RX \cos RZ$
$C_{23} = \cos RX \sin RY \sin RZ - \sin RX \cos RZ$
$C_{31} = -\sin RY$
$C_{32} = \sin RX \cos RY$
$C_{33} = \cos RX \cos RY$

The next step is to express the accelerations $\ddot{x}_G, \ddot{y}_G, \ddot{z}_G, \ddot{RX}, \ddot{RY}$ and $\ddot{RZ}$ for given outer forces and moments as they may occur during a collision.

In order to facilitate a classical mechanical computational procedure, so-called added or hydrodynamic masses and moments of inertia are specified. In this manner it is taken into account that also the surrounding water undergoes accelerations whenever the vessel does.

For translatory movements in the direction of the x_A-axis it can be assumed that the acceleration will be equal to the outer force F_{xA} in the x_A-direction divided by the sum m_{xA} of the mass of the vessel and the added mass. Analogue assumptions are introduced for translatory movements in the direction of the y_A- and z_A-axis. Generally, m_{xA} is only a few per cent larger than the mass of the vessel whereas m_{yA} and m_{zA} can be twice the mass of the vessel. In the fixed frame of reference these equations can be written

$$\begin{bmatrix} F_x \\ F_y \\ F_z \end{bmatrix} = \begin{bmatrix} m_{11} & m_{12} & m_{13} \\ m_{21} & m_{22} & m_{23} \\ m_{31} & m_{32} & m_{33} \end{bmatrix} \begin{bmatrix} \ddot{x}_G \\ \ddot{y}_G \\ \ddot{z}_G \end{bmatrix}$$

where the non-diagonal elements generally are non-zero and only vanish for RX = RY = RZ = O (or $m_{xa} = m_{ya} = m_{za}$).

For rotational movements it can be assumed that the vessel's centre of the ellipsoid of inertia coincides with the vessel's centre of gravity and that the principal axes of the ellipsoid of inertia coincide with the x_A-, y_A- and z_A-axis. In analogy with the treatment of translatory movements, it is assumed that the angular acceleration around the x_A-axis is equal to the moment M_{xA} of the vessel's moment of inertia and the added moment of inertia. Analogue assumptions are introduced for angle accelerations around the y_A- and z_A-axis. If the generally valid vectorial moment equation is projected on the directions of the x_A-, y_A- and z_A-axis, the following equations are obtained

$$\begin{aligned} I_{xA} \dot{\Omega}_{xA} + (I_{zA} - I_{yA}) \Omega_{yA} \Omega_{zA} &= M_{xA} \\ I_{yA} \dot{\Omega}_{yA} + (I_{xA} - I_{zA}) \Omega_{zA} \Omega_{xA} &= M_{yA} \\ I_{zA} \dot{\Omega}_{zA} + (I_{yA} - I_{xA}) \Omega_{xA} \Omega_{yA} &= M_{zA} \end{aligned}$$

where the angular velocity reads:

$$\begin{aligned} \Omega_{xA} &= \dot{RX} - \sin RY\ \dot{RZ} \\ \Omega_{yA} &= \cos RX\ \dot{RY} + \sin RX \cos RX\ \dot{RZ} \\ \Omega_{zA} &= \sin RX\ \dot{RY} + \cos RX \cos RY\ \dot{RZ} \end{aligned}$$

From these equations it is seen that $\ddot{RX}$, $\ddot{RY}$ and $\ddot{RZ}$ can be determined from $\dot{\Omega}_{xA}$, $\dot{\Omega}_{yA}$ and $\dot{\Omega}_{zA}$ which in turn can be determined from the outer moments.

As long as all outer forces and moments can be described as function of the vessel's instantaneous position (6 parameters) and velocity (6 parameters) - possibly with some knowledge of the prehistory such as deformations - the instantaneous accelerations can be found from the above described equations. Numerical integration can be carried out with only little computational effort and thereby provide the time history of a collision event of interest.

The added masses depend on frequency as described by Motora et al (1971). Rather than selecting a single representative value for given collision circumstances, the variation of the added masses and moment of inertia during the collision may be computed by a strip method where the forces acting on each section of the vessel are described by means of unit response functions, see Petersen (1980). Fig. No. 1 from this reference shows the ratios between the added mass (momentum of inertia) and the vessels's mass (momentum of inertia) for sway and yaw as function of cyclic frequency ω.

L (LENGTH) = 116m   B (BEAM) = 19m   T(DRAUGHT) = 6.9m
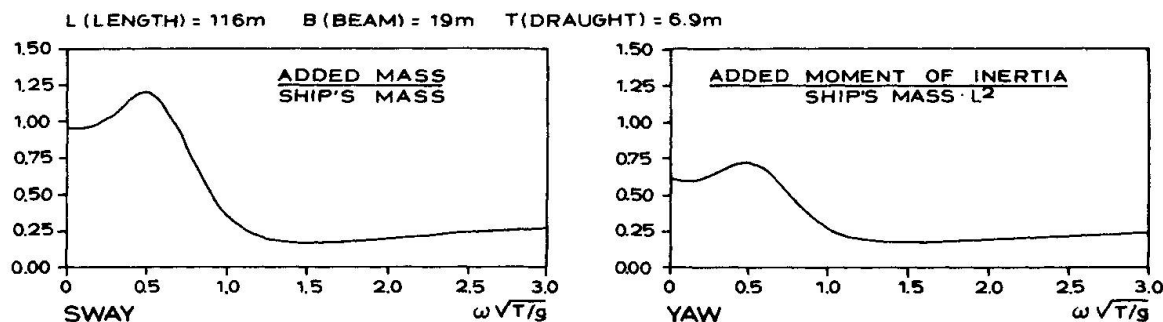

Fig. No. 1   Added Mass and Moment of Inertia for Sway and Yaw.

It is seen that these ratios are significantly larger for low-frequency disturbances - such as collisions between ships and structures - than they are for high-frequency disturbances. The proper assessment of these characteristics for sway and yaw is important when evaluating the deflecting characteristics of a protective structure and when evaluating the kinetic energy of a vessel drifting sideways (swaying) into a bridgepier or platform.

Following Salvesen (1970) hydrodynamic damping forces and moments can be assumed to be proportional to the six translatory and rotational velocities. Hydrodynamic restoring forces and moments can be assumed to be proportional to the displacement z_G, RX and RY; also a cross-coupling term between heave and pitch (z_G and RY) should be included.

The hydrodynamic damping forces are not of much importance for the evaluation of collision circumstances. The restoring forces play a more crucial role as they generally tend to bring the vessel back to a position with large contact forces and thereby transform the kinetic energy in a destructive manner with only little energy being transformed into potential energy expressed in terms of z_G, RX and RY.
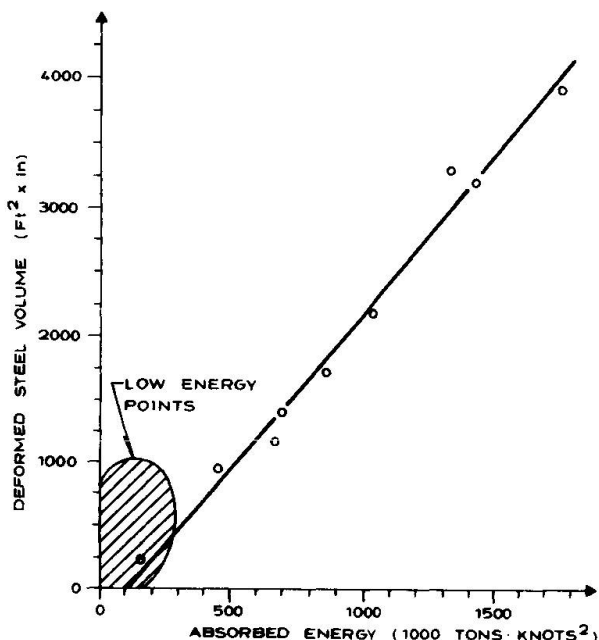
3.   COLLISION FORCES

Fig. No. 2   Minorsky's Empirical
Relationship between
Impact Energy and De-
formed Volume of Steel.

Minorsky (1959) derived a simple empirical relationship between absorbed energy and the volume of steel in the damaged portions of decks, longitudinal bulkheads and shell plating, see Fig. No. 2. For a given vessel an estimate of the load deformation curve can be reached from this relationship, e.g. as shown by Olnhausen (1966). Also, this simple relationship agrees surprisingly well with the experimental results of Woisin (1971) who rammed ship bows in scale 1:7.5 and 1:12 into strong protective structures for reactors in nuclear powered ships. Following Woisin, typical values of the average impact force to be reached during head-on collisions will range from 200-300-400 MN for 50-100-200 10^3 DWT vessels. In the very beginning of the collision, impact forces reaching twice these values may be experienced within short durations, say 0.1 sec. For a given size of vessel the impact force may deviate from the above typical figures by approx. 50 per cent.

Model results like those of Woisin (1971), Ando and Arita (1976), Arita et al (1977), Nagasawa el al (1977), and Iwai et al (1980) provide insight to the relationship between the load-penetration curve and the structures of the ship bow. In theoretical models the structures of the vessel can be decomposed into simpler structural elements. Reckling (1976,1977) obtained accurate agreement with Woisin's experiments by distinguishing between three major types of plastic damage : accordion-shaped folding of longitudinally stressed plating, tearing open of longitudinally stressed plating where the collision opponent intrudes, and tearing open of laterally stressed plating due to large membrane strains. Of special relevance for ship collisions against bridge piers is Reckling's calculation of the instability load of all the longitudinally stressed plating (decks) in a striking ship bow. The computed forces agreed within 10 to 20 per cent of the measured impact forces in the tests where the ship bow was completely damaged. Jones (1979) presents a litterature survey on these aspects of ship collisions.

4. RIGID VESSEL AGAINST RIGID STRUCTURE

The collision between a vessel and a
sloping structure may as a first ap-
proximation be treated as a collision
between two rigid bodies, the vessel
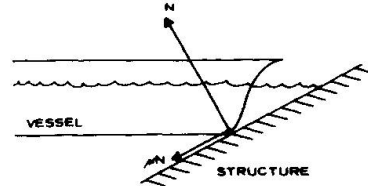responding to outer forces as out-
lined in Chapter 2. This is done by

Fig No.3 Definition Sketch.

1) computing the impulses I (perpendicular to the slope) and μI
   (directed opposedly to the projected track on the slope of the vessel's
   collision point) which change the velocity of the vessel's collision
   point to become parallel to the slope.

2) computing the forces N and μN which accelerate the vessel in such a manner
   that the vessel's collision point remains at the slope (or ultimately loose
   contact).

The kinematic conditions from which the collision impulses and -forces are
computed lead to simple linear equations which can be solved by standard
methods. Computations of the entire collision providing time series of the
collision force and the vessel's displacements and velocities can then be car-
ried out for the full three-dimensional case as outlined in Chapter 2. The
assumption of vessel and structure being rigid is only valid for some low-
energy collisions or high-energy collisions with very small contact forces
acting over long distances. However, the results which can be obtained with
this assumption will provide upper- or lower-bound values for a number of
parameters such as e.g. maximum potential energy in heave, roll and pitch
(z_G, RX, RY) and maximum vertical displacement of vessel's bow. Such values can
prove useful when evaluating the results and strategy of more detailed
investigations.

5. DEFORMABLE VESSEL AGAINST RIGID STRUCTURE

If, in a collision scenario like that shown in Fig. No. 3, the sloping
protective structure is a concrete structure with sufficient overall strength,
the vessel will be the weaker part. In that case the simple kinematic condition
of Chapter 4 has to be replaced by a load-penetration curve for the plastic
deformation of the vessel.

Fuchs et al (1978) assumed the contact force to be proportional to the contact
area with a velocity directed towards the sloping structure. The frictional
force was computed as outlined in Chapter 4, μ=0.25 was applied. In order to
keep track of the deformations, the vessel was sliced (computationally) in the
longitudinal directions, and for each segment the individual contributions to
the total outer force and moment were determined. The motions of the vessel
were then determined in accordance with the theory presented in Chapter 2.
Simulations were carried out for different combinations of vessel's speed,
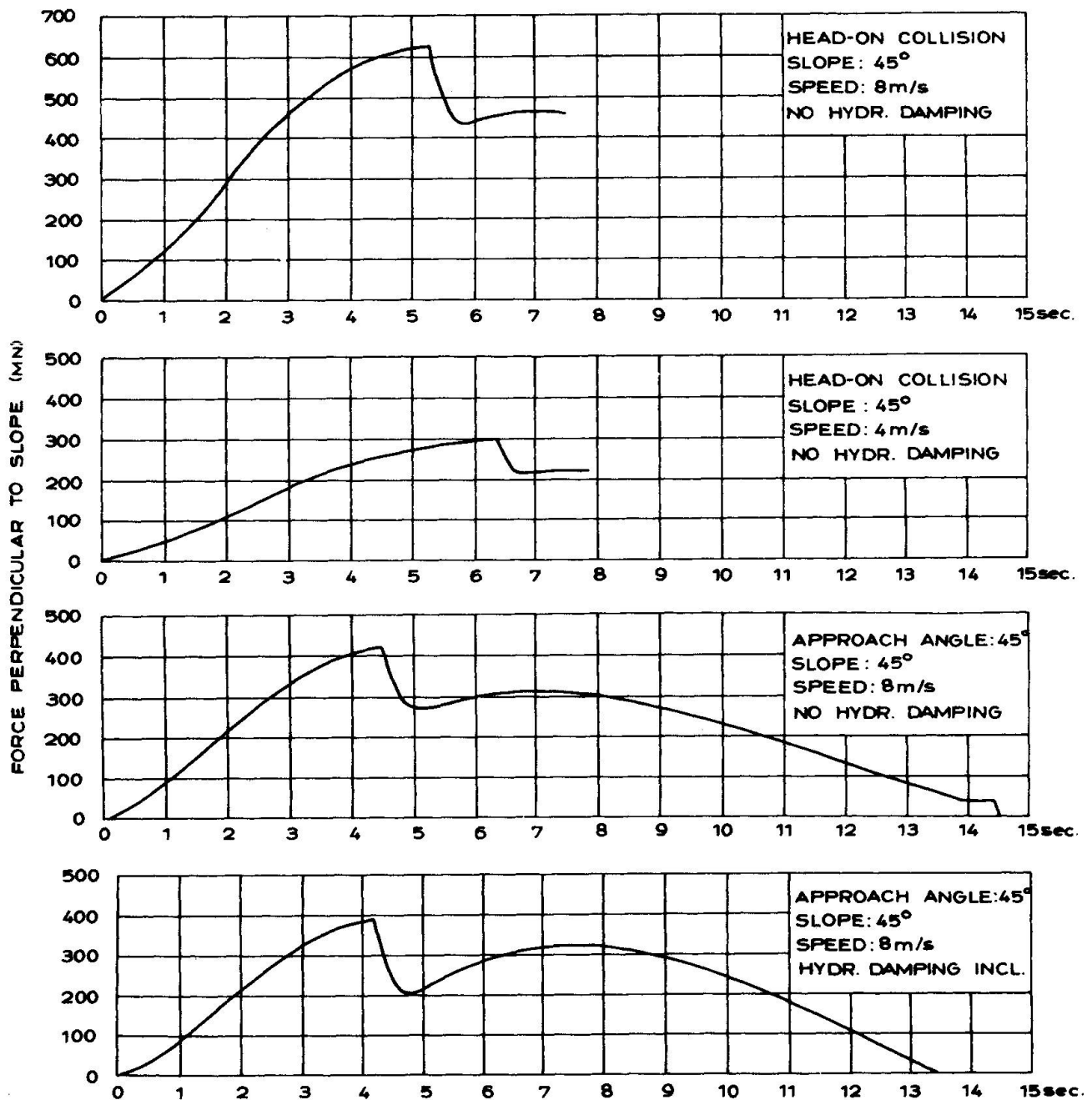size, strength, angle of approch and for different slope angles.

Fig. No. 4   Collision Forces for a fully Loaded 250,000 DWT Tanker
Colliding with a Rigid Slope (1:1).

Fig. No. 4 shows four time series of the collision force perpendicular to the slope for a fully loaded 250,000 DWT tanker for which the contact-force area ratio in all cases is 4 10^5 N/m^2. The two upper time series refer to head-on collisions with initial vessel speeds of 8 m/s and 4 m/s, respectively. The two lower time series refer to obliquely incoming (45°) vessels with an initial speed of 8 m/s and with hydrodynamic damping excluded and included, respectively.

For a slope angle of 45 degrees and a friction coefficient of 0.25, the horizontal force equals 88 per cent of the force perpendicular to the slope for head-on collisions. Except for this constant ratio the two upper curves show how the vessel's initial momentum (M_{xA} times initial vessel speed) is brought to zero by the time integrated horizontal force i.e.

$$m_{xA} \ V_{init} \ = \int F_{Horizontal} \ dt$$

The fastgoing vessel (upper curve) is more rapidly damaged and the maximum collision force, although appr. two times larger, is reached earlier than in the case for the more slowly moving vessel. The durations of these collisions events are almost identical.

For the obliquely incoming vessel, see the lower two curves of Fig. No. 4, the duration of the collision is considerable larger. This is so because of the large added mass and moment of inertia for sway and yaw. However, it is important to note that the maximum collision force is only appr. two-third of that experienced for the head-on collision with the same initial speed of vessel.

By comparing the two lower curves of Fig. No. 4 it is seen that the inclusion of the hydrodynamic damping terms are not of great significance.

6. RIGID VESSEL AGAINST DEFORMABLE STRUCTURE

In case the protective structure is a rubble mound structure, the vessel will be the stronger part - at least in the initial stages of a collision. In this chapter the collision characteristics of such protective structures will be discussed in rather detail. For the Great Belt Bridge Project, hydraulic model tests were carried out by the Danish Hydraulic Institute in order to provide insight to the dynamics of such collisions.

6.1 Study Program

A first series of tests was carried out for vessels colliding with an (infinitely) long rubble mound slope with a horizontal berm and a second series of tests were carried out for rubble mound islands with a horizontal berm. The purpose of the first series of tests was to provide insight to the stopping and deflecting capabilities of a rubble mound slope as function of
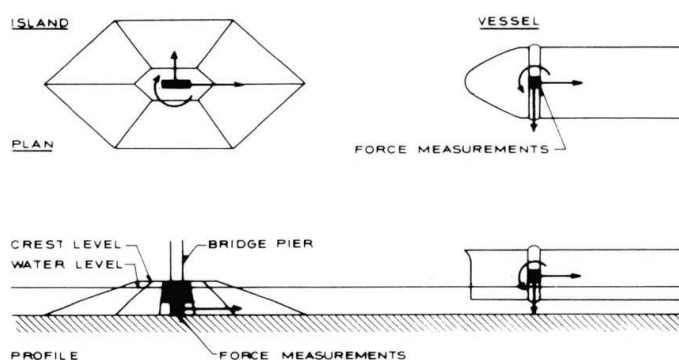
- shape of ship bow
- vessel's angle of approach
- speed of vessel
- vessel's size and load condition (draught)
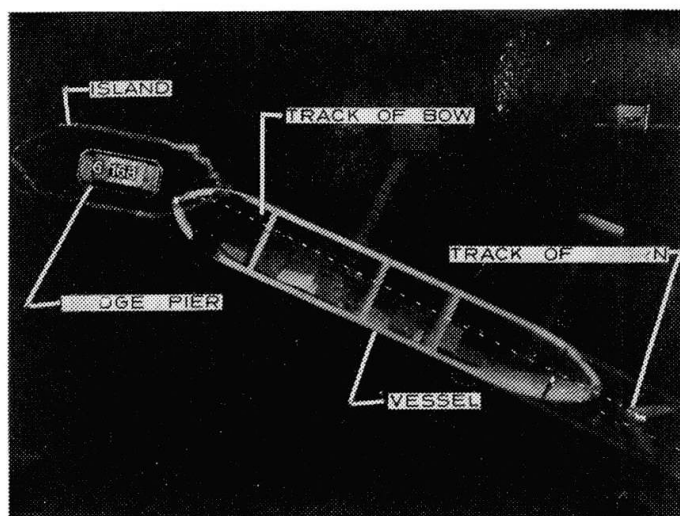- level of berm.

The purpose of the second series of tests was to test proposed configurations of protection island and thereby contribute to the design of protection islands with optimum deflecting and stopping capabilities.

The results of investigations in the areas of naval architecture and soil mechanics were applied in the formulation of a deterministic mathematical model following the theory outlined in Chapter 2. The purpose of developing such a model was to interrelate the results of hydraulic and soil mechanic model tests and to predict collision events not covered by the hydraulic model tests.

6.2 Hydraulic Model Set-up

Most tests were performed with a 250,000 DWT and a 150,000 DWT tanker. Some were carried out with a 50,000 DWT container ship. Altogether approximately 500 tests were performed. The model length scales were 1:94 and 1:79. Froude-scaling was applicable. The rubble mound slopes and islands consisted of uniform sharply crushed stones, corresponding to 400 kg stones in nature. The slopes were in all tests 1:1.5 and the berms were horizontal.

The tracks of the vessels were registered by a camera which was mounted above the protection structure. Flashing lights on the bow and the stern clearly indicated the tracks and the velocities of these parts of the vessel, see Fig. No. 5.

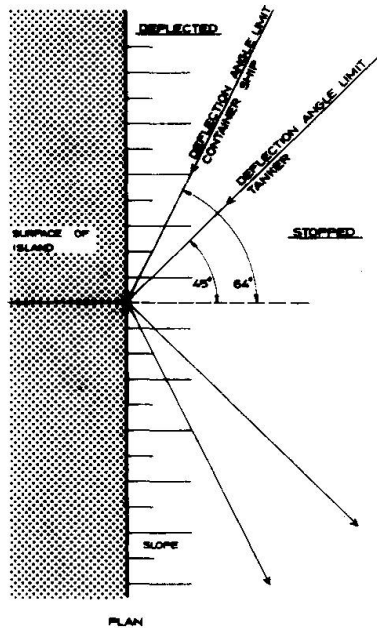Further, the speed was measured by a photo cell right before the collision.

The vessel could move freely during the collision.

Fig. No. 5 Hydraulic Model Set-up.

The model ship bow was cut off and reconnected to the hull through dynamometers. In this way three force components and two moment components were measured simultaneously during the collision. The bridge pier was fastened to the floor of the laboratory through a dynamometer, too. Two force components and one moment component were measured simultaneously.
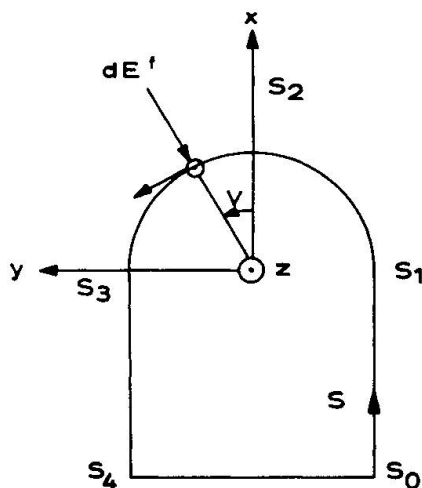
6.3   Collisions with Rubble Mound Slopes

From the first series of model tests the influence of approach angle and shape of ship bow is summarized in Fig. No. 6.

In the case of a head-on collision the vessel penetrates into the protection slope until it is ultimately stopped. An obliquely incoming vessel may be deflected by the protection structure and continue with decreased speed. The limiting approach angle determining the favourable deflecting behaviour depends on the shape of the ship bow. The long narrow bow of a container ship almost steers the ship into the protection slope from where it will only escape for courses which are rather parallel to the structure. The tanker has a rounded bow and is deflected even for approach angles of 45° with the alignment of the structure.

Fig. No. 6   Deflective Characteristics
            of Rubble Mound Slopes.

The soil mechanic tests were carried out for tanker bows only as they were considered the more relevant for the Great Belt Bridge Project. In the following all results refer to vessels with tanker bow shapes. From the soil mechanic tests the following formulation was adopted for modelling the contact force for all contact areas of the vessel having a velocity component towards the structure.
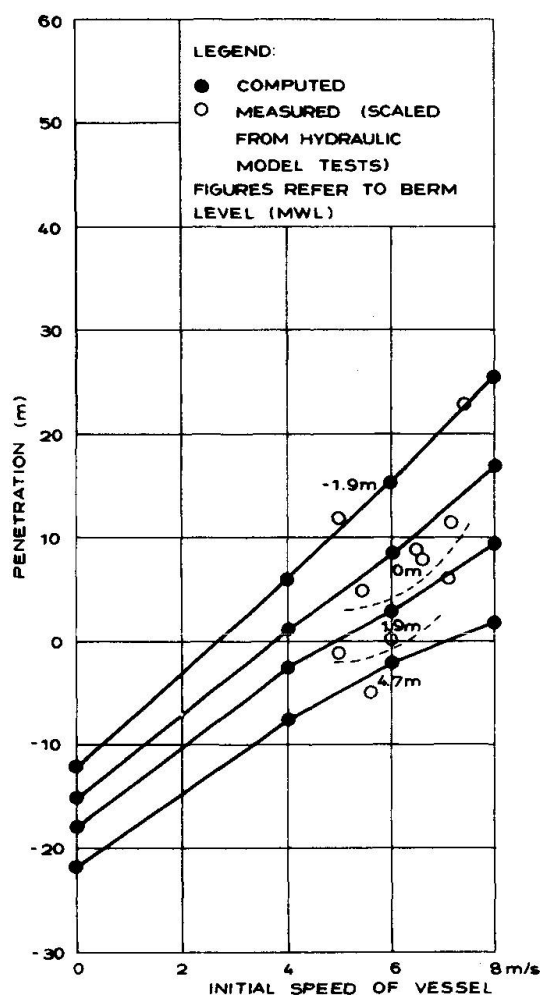

$$F_x = \int_{s1}^{s3} (\cos v + \mu \sin^3 v) \, dE^f$$

$$F_y = \int_{s1}^{s2} (\sin v + \mu \cos v \sin^2 v) \, dE^f$$
$$+ \int_{s2}^{s3} (\sin v - \mu \cos v \sin^2 v) \, dE^f$$

$$F_z = \int_{s1}^{s3} \mu \cos^2 v \, dE^f$$

Fig. No. 7   Definition Sketch. Contact Forces.

A semi-analytical expression for the force component dE^i was derived by the Danish Geotechnical Institute (1978). This expression took into account the vertical depth of penetration, the effect of the berm on earth pressure in the sloping part of the structure, the additional pressure from displaced material, and the reduction in contact force near corners of the protection island.

The outer force and moment was computed by integrating the above expression along the vessel's bow.

Fig. No. 8 shows computed and measured penetrations for a 250,000 DWT tanker with a draught of 10 m, which collides head-on with a rubble mound slope (1:1.5). The influence of different collision speeds and berm levels was examined. The penetration is measured from the intersection between the slope and the berm. For vessel speeds up to 8 m/s good agreement between measured and computed penetrations was obtained.

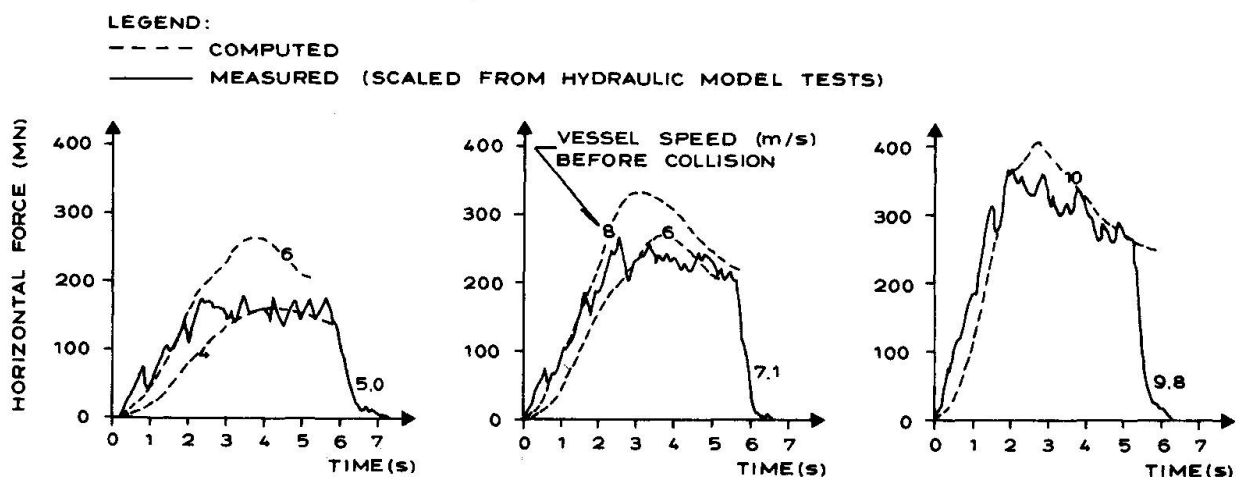Fig. No. 8   Measured and Computed Penetrations for a 250,000 DWT Tanker, Draught 10 m. Slope (1:1.5).

LEGEND:

– – – – COMPUTED

———— MEASURED (SCALED FROM HYDRAULIC MODEL TESTS)

Fig. No. 9   Computed and Measured Collision Forces for a 250.000 DWT Tanker, Draught 10 m. Berm Level 1.9 m (MWL).

Fig. No. 9 shows a comparison between computed and measured horizontal collision forces in the case with a berm level of 1.9 m above the mean water level (MWL). It is seen that close agreement has been obtained for the entire collision event for a wide range of collision speeds. As discussed in Chapter 5 these horizontal force-time diagrams for head-on collisions directly show how the initial momentum of the vessel is brought to zero, in these cases by a fairly constant force which is reached when most of the ship bow below the berm level is involved in the collision.

Fig. No. 10 shows comparisons between measured and computed penetration distances for obliquely incoming vessels, again for a 250,000 DWT tanker with a draught of 10 m.
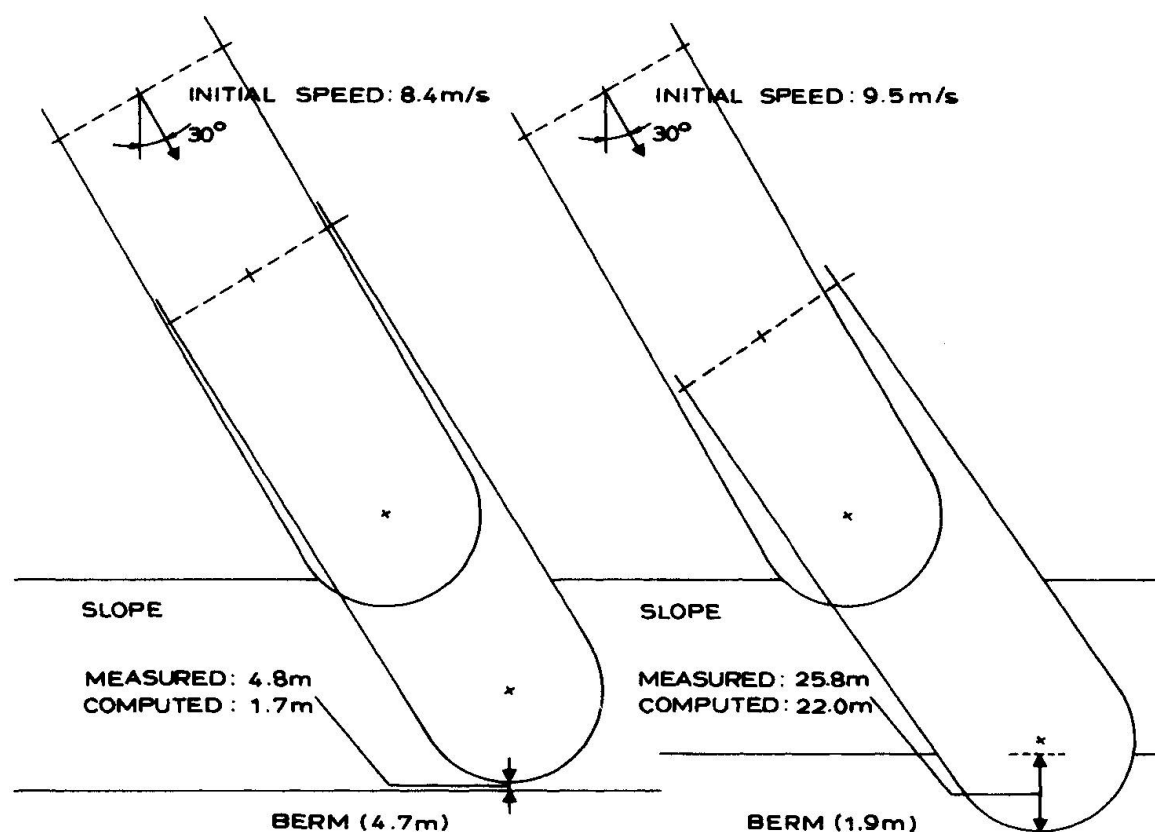

Fig.No. 10   Measured and Computed Penetrations for an Obliquely Incoming 250,000 DWT Tanker, Draught 10 m.

6.4 Collision with Rubble Mound Islands

Fig. No. 11 illustrates that also the deflecting characteristics of a protective island can be computed in close agreement with measurements. This supports the idea of modelling contact forces between vessels and structures in rather detail as it was done here with a complex distribution of the contact pressure along the ship bow.

It is also seen from Fig. No. 11 (and documented in detail by the hydraulic model tests) that vessels which approach the protection island from the approach angle here shown are almost inevitably deflected.
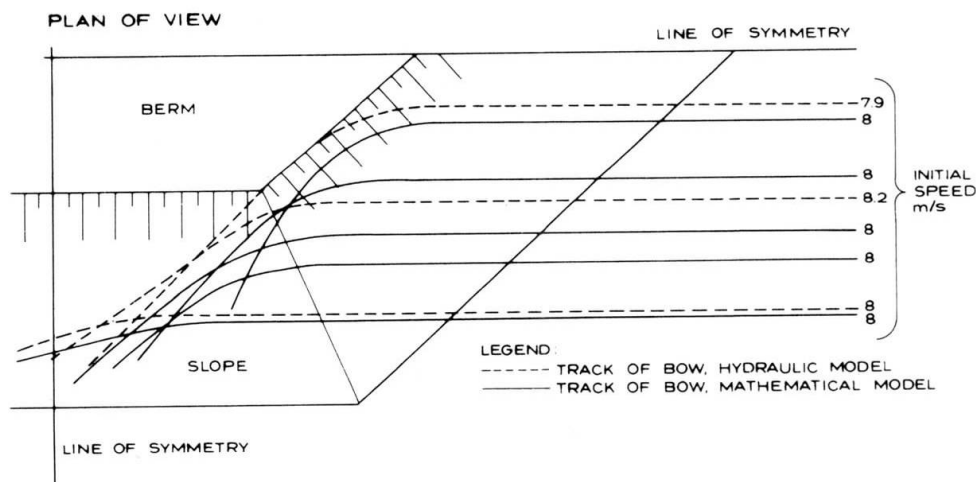

Fig. No. 11   Measured and Computed Bow Tracks for a 250,000 DWT Tanker, Draught 10 m.
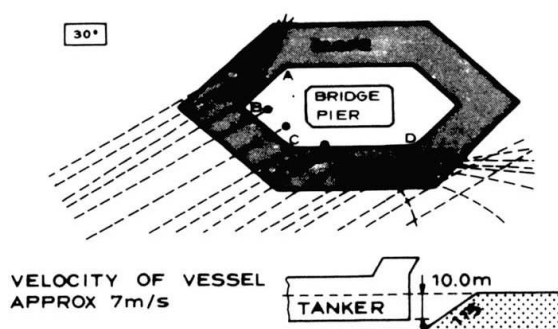

Fig. No. 12 shows that the important deflective characteristics are maintained for vessels approaching under a more infavourable approach angle.

Fig. No. 12   Bow Tracks for 250,000 DWT Tanker, Draught 10 m, Colliding with a Protection Island.

Fig. No. 13 summarizes the significance of having structures with optimal deflective characteristics. Not only the horizontal collision forces between the vessel and the structure decreases rapidly when the vessel is deflected, but the horizontal force ultimately transferred to the bridge pier is further reduced.

Consequently, the probability of occurence of a given impact force can be significantly reduced by protective rubble mound structures. Such protective structures can therefore be considered a realistic type of solution for reaching an acceptable risk level for structures exposed to high-energy collisions.
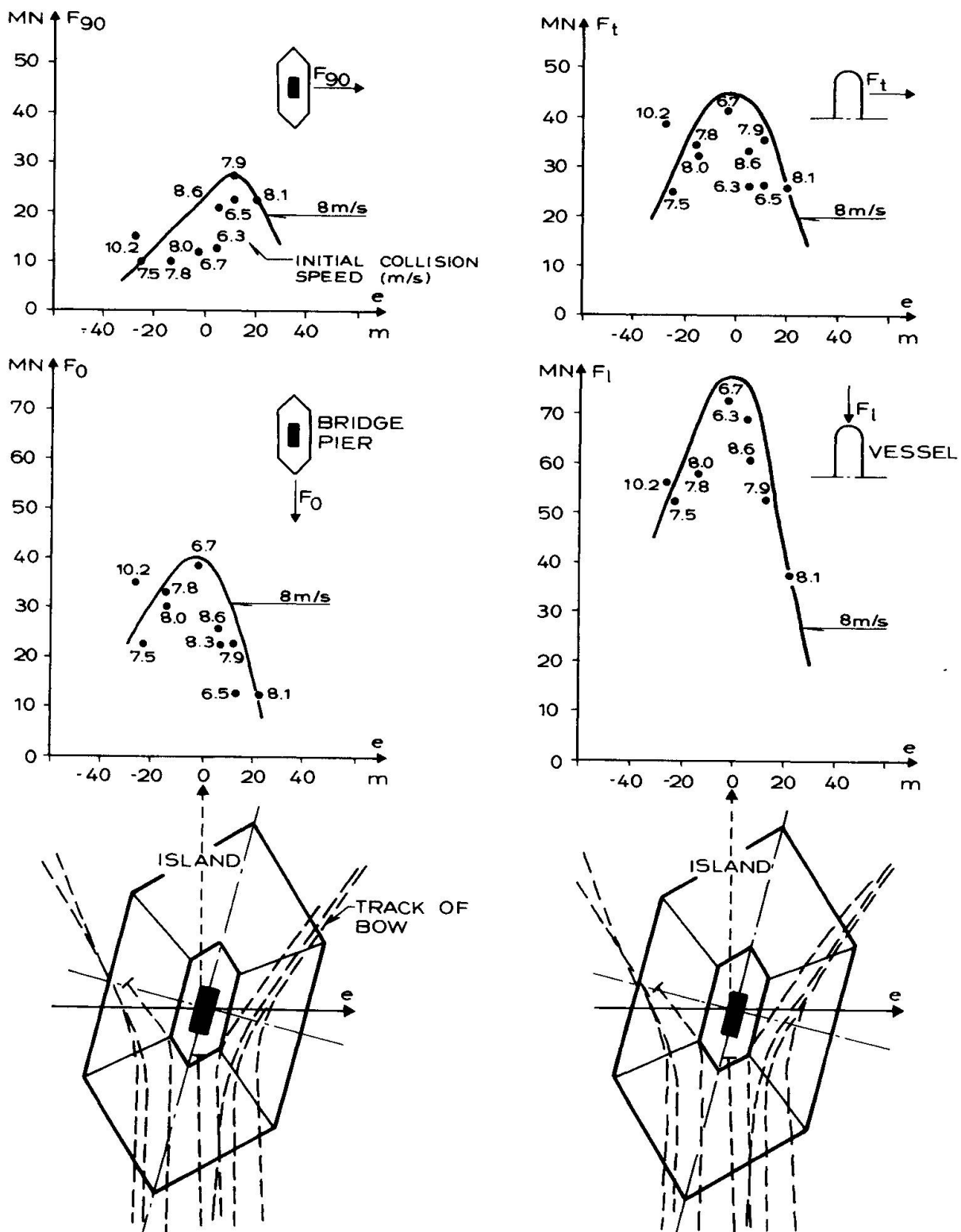
Fig. No. 13 Measured Forces in Bridge Pier and Vessel for 150,000 DWT Tanker, Draught 10 m, Colliding with Rubble Mound Island.

6.5   Other Applications

It could be mentioned that the computational procedure outlined above has been applied for the evaluation of penetration depths from ships grounding in the Danish Belts and that the results so obtained were used for deciding on trenching depths and spacing between marine gas pipelines, presently being laid in the Danish Belts.

7.   DEFORMABLE VESSEL AGAINST DEFORMABLE STRUCTURE

The more general formulation of the collision problem operates with the load-deformation curves for both vessel and structure. Such formulations exist for two colliding vessels and e.g. also for low-energy collisions between a swaying vessel and an offshore platform, Petersen and Pedersen (1980).
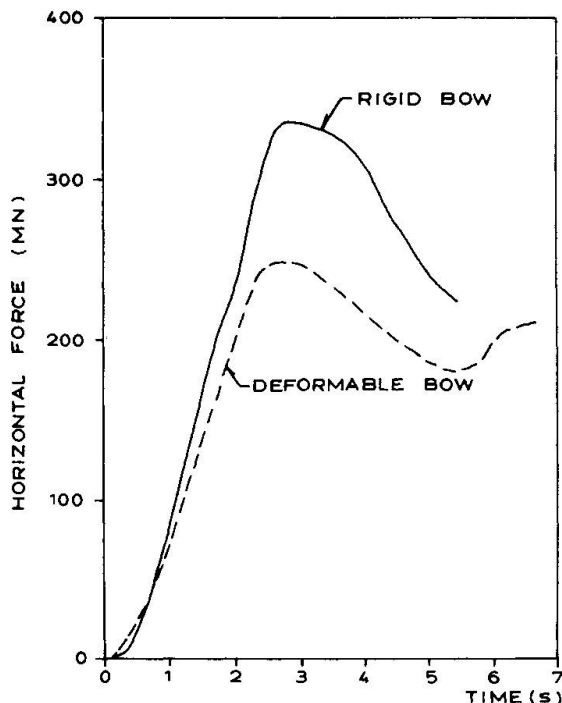
For high-energy collisions between a vessel and a rubble mound slope, Fuchs et al (1978) combined the assumptions presented in Chapter 5 and 6 for the vessel and the protective structure, respectively. This leads to a simplified description in which the vessel initially penetrates as a rigid body, but at a certain depth below the structure's surface, the contact pressure exceeds the strength of the vessel which in turn is deformed rather than the structure. This formulation therefore leads to smaller collision forces than those presented in Chapter 6. This is demonstrated in Fig. No. 14 which shows the computed horizontal collision forces for a head-on collision between a 250,000 dwt tanker, draught 10 m, and a rubble mound structure with a berm level of 1.9 m (MWL). The vessel was assumed to be rigid in one case and to be deformable with a contact force/area ratio of $5 \cdot 10^5$ N/m^2 in the second case.

Fig. No. 14   Comparison between computed Horizontal Forces for Rigid and Deformable Ship Bows

On one hand, the deformation of the vessel leads to smaller collision forces than those measured and computed for the rigid vessel. On the other hand, the upper part of the ship's bow will move a greater distance over the berm and thereby increase the probability of direct contact between the vessel and the main structure.

8. CONCLUSIONS

The consequences of a collision between a vessel and a protective structure are determined by many parameters such as the speed, course, size, bow shape and hull stiffness of the vessel and the strength and geometrical shape of the protective structure.

These parameters can all be taken into account by applying a deterministic description which is based on classical mechanical principles.

In case existing knowledge on some of the subprocesses of a collision is insufficient, model tests can be planned and interpreted with great economy of effort when the results are to be integrated with a deterministic formulation into one single body of knowledge. In this paper this point is illustrated in detail by results obtained for the planning of the now postponed Great Belt Bridge (Denmark).

9. ACKNOWLEDGEMENTS

The authors wish to thank Statsbroen Store Baelt (SSB) for permission to publish this paper and to use results from other consultants of SSB, notably Storebæltsgruppen, consulting engineers and planners, the Ship Research Laboratory, The Danish Geotechnical Institute and the Danish Hydraulic Institute.

10. REFERENCES

ANDO, N. and ARITA, K., A Study on the Strength of Double-Hull Structures in Collision, (in Japanese), Trans. Soc. of Naval Arch. of Japan, 139, 147-156, 1976.

ARITA, M., ANDO, N., ARITA, K., Study on the Structural Strength of Ships in Collision, Conference on Fracture Mechanics and Technology, Hong Kong, 1977.

DANISH GEOTECHNICAL INSTITUTE, Geotekniske Modelforsøg. Rapport nr. 2 med bilag 37-54, (in Danish), 1978.

FUCHS, J. U., HAVNØ, K., TRYDE, P., BRINK-KJÆR, O., Skibsstød mod faste konstruktioner og sandøer, (in Danish), Institute of Hydrodynamics and Hydraulic Engineering, Technical University of Denmark, 1978.

IWAI, A., NAGASAWA, H., ODA, K., SHOJI, K., Ship-bridge pier protective systems, proc. Coastal Engineering Conference, 1980.

JONES, N., A litterature survey on the collision and grounding protection of ships, U. S. Coast Guard Headquarters, Washington D.C., 1979.

MINORSKY, V. U., An Analysis of Ship Collisions with Reference to Protection of Nuclear Power Plants, J. Ship Research, 3, 1-4, 1974.

MOTORA, S., FUJINO, M., SUGIURA, M., SUGITA, M., Equivalent Added Mass of Ships in Collisions, Selected Papers from the Journal of the Society of Naval Architects of Japan, 7, pp. 138-148, 1971.

NAGASAWA, H., ARITA,K., TANI, M., OKA,S., A Study on the Collapse of Ship Structure in Collision with Bridge Piers (in Japanese), Trans. Soc. of Naval Arch. of Japan, 142, 345-354, 1977.

OLNHAUSEN, M. VON, Påsegling av Bropelare, Teknisk Tidsskrift, (in Swedish), Hæfte 17, 1966.

PETERSEN, M. J., Dynamics of Ship Collisions, DACAMM, Report No. 185, Technical University of Denmark, July 1980.

PETERSEN, M. J., and PEDERSEN, P. T., Collisions between Ships and Offshore Platforms, proc. Offshore Technology Conference, 1981.

RECKLING, K. A., Beitrag der Elasto- und Plastomechanic zur Untersuchung von Shiffskollisionen, (in German), Jahrbuch der Schiffbautechnischen Gesellschaft, 70, 443-464, 1976.

RECKLING, K. A., On the Collision Protection of Ships, Int. Symp on Practical Design in Shipbuilding, Soc. of Naval Architects of Japan, Tokyo, 129-134, 1977.

SALVESEN, N., TUCK, E. O., FALTINSEN, O., Ship Motions and Sea Loads, S.N.A.M.E. Transactions, 1970.

WOISIN, G., Schiffbauliche Forschungsarbeiten für die Sicherheit Kernenergigetriebener Handelsshiffe, (in German), Jahrbuch der Schiffbautechnischen Gesellschaft, 65, 225-263, 1971.

Means of Reducing the Consequences of Ship Collisions with Bridges and Offshore Structures

Ouvrages de protection des ponts et des constructions maritimes contre des collisions de bateau

Beschränkung der Auswirkungen eines Schiffsanpralls gegen Brücken und Meeresbauten

Reiner SAUL
Senior Superv. Eng.
Leonhardt, Andrä und Partner GmbH
Stuttgart, Fed.Rep.of Germany

Holger SVENSSON
Senior Project Eng.
Leonhardt, Andrä und Partner GmbH
Stuttgart, Fed.Rep.of Germany

Reiner Saul, born in 1938, Dipl.-Ing. of Civil Engineering, Univ. of Hannover in 1963. Four years with a steel contractor, since 1971 senior supervising engineer with Leonhardt, Andrä und Partner. He was responsible for the design, technical direction and checking of numerous long-span bridges, including also major rehabilitation works.

Holger Svensson, born in 1945, Dipl.-Ing. of Civil Engineering, Univ. of Stuttgart 1969. After two years with a general contractor he joined Leonhardt, Andrä und Partner, where he works on all aspects of the design and construction of long-span, mainly cablestayed bridges, including their protection against ship collision.

SUMMARY

Possible structural measures to protect bridges and offshore structures against ship impact are described and their efficiencies are evaluated. Such measures are floating systems, systems using piles, fixed or sliding dolphins with or without fenders and protective islands. Finally conclusions are drawn for the planning of new bridges taking into account their protection against ship collision.

RÉSUMÉ

Les ouvrages de protection des ponts et des constructions maritimes contre une collision de bateau sont décrites et examinées du point de vue de leur efficacité. On y traite des systèmes flottants, des systèmes sur pieux, des îlots artificiels. Des indications fondamentales sont données pour le projet de nouveaux ponts tenant compte de leur protection contre une collision de bateau.

ZUSAMMENFASSUNG

Es werden konstruktive Möglichkeiten, um Brücken und Meeresbauten vor den Folgen eines Schiffsanpralls zu schützen, beschreiben und auf ihre Brauchbarkeit hin untersucht. Behandelt werden schwimmende Systeme, Systeme suf Pfählen, feste und bewegliche Kreiszellen mit oder ohne Fender und künstliche Aufschüttungen. Abschließend werden grundsätzliche Hinweise zum Entwurf neuer Brücken, unter Berücksichtigung des Schutzes gegen Schiffsanprall, gegeben.

1. INTRODUCTION

Over the recent years a constant increase of shipping accidents with bridges and offshore structures took place. The reasons for these are, on the one hand, attributed to the increase in shipping traffic and the size of the ships, Figure 1, on the other hand, to the fact that more bridges are being built in deep water and on poor ground. The protection of bridges is therefore becoming increasingly more important.

In the U.S.A. alone are about 100 major bridges across principal shipping lanes, 11 of which were involved in major ship collisions in recent years, which besides considerable material costs also exacted a toll of nearly 100 human lives. The damages stemming from ship collisions thereby exceed those connected with wind, waves, earthquakes or increased loads, [2].

Experience indicates that it will not be possible to avoid collisions completely, but it is possible to reduce their consequences: the damage to the

Fig.1   Development of merchant marine traffic. From [1]

struck structure must not lead to its collapse and to loss of human life and the ship must not sink or be damaged in such way that its cargo, e.g. oil, pollutes the environment.

Protective installations, therefore, should protect the structure as well as the ship. This paper deals only with protective installations for the structure.
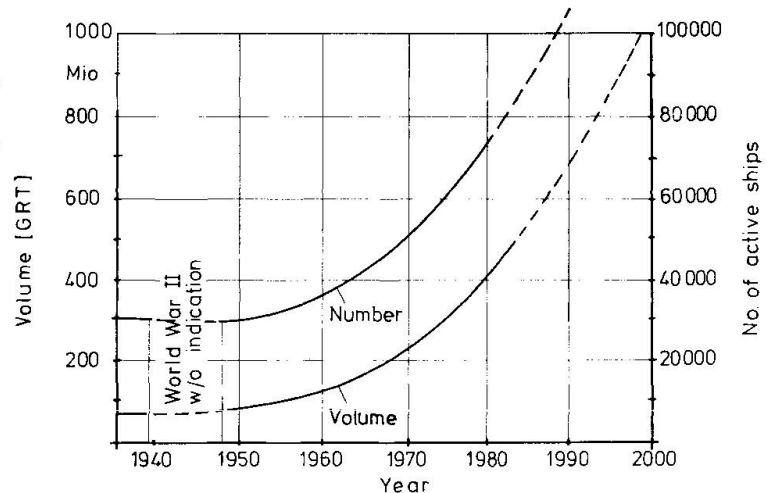
2. COLLISION ENERGY AND IMPACT FORCES

The kinetic energy of a ship moving straight forward amounts to

$$E_K = \frac{1}{2} \cdot m_1 \cdot 1.05 \cdot v_0^2$$

with m_1 ship's mass
        1.05   factor for additional hydrodynamic mass
        v_0 ship's speed .

The collision energy ΔE to be transformed by the structure hit (in the following simplified called pier) and/or the ship into another energy form is hence

$$\Delta E = \eta \cdot E_K$$
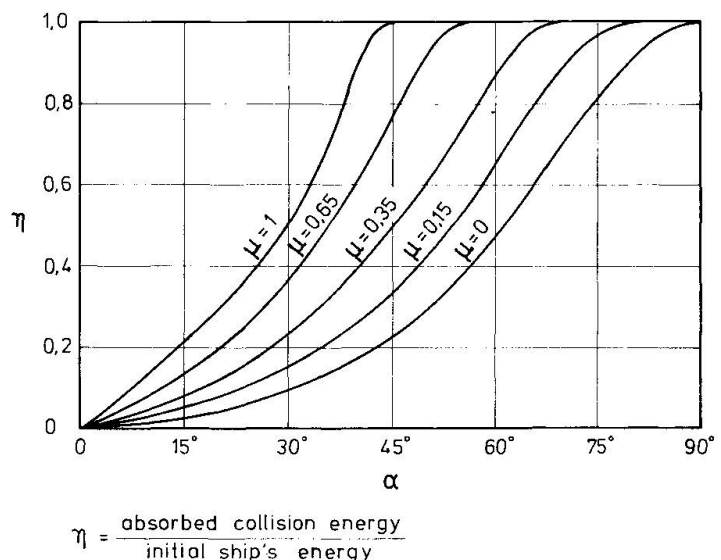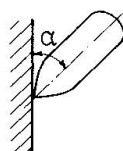
as shown in [3], see Figure 2.

Fig.2   Part of collision energy η to be absorbed by the ship and/or pier in relation to the collision angle α and the friction μ

$$\eta = \frac{\text{absorbed collision energy}}{\text{initial ship's energy}}$$

Friction μ

Steel - steel   ~ 0,15
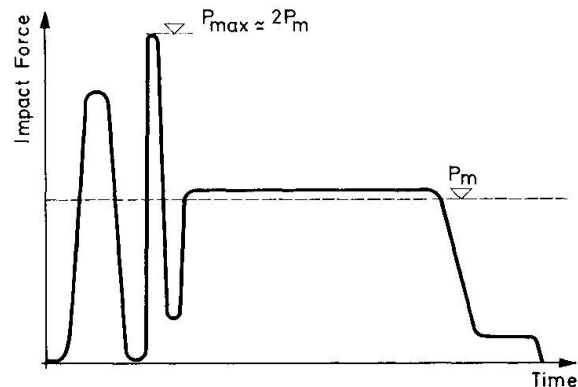Steel - concrete ~ 0,35
Steel - wood   ~ 0,65

The impact force created by a right-angle collision of a ship against a stiff pier has been deduced by Woisin from measurements in collision tests.

From those tests it was concluded that the medium impact force

$$P_m = \frac{\Delta E}{a} \quad \text{(a: length of damage)}$$

is approximately constant during the collision. The maximum impact force P_{max} increases at the beginning of the impact for approximately 0.1 - 0.2 seconds to double the amount of P_m, Figure 3.

Fig.3 Impact forces from a collision test between the bow model of the passenger liner T/S Bremen against the side model of the N/S Otto Hahn, Test No.1 of the GKSS. From [4]

For bulk carriers it was concluded that the effective maximum impact force for an impact against a stiff pier follows in first approximation the formula

$$P_{max} \approx 0,88 \sqrt{dwt} \quad \pm 50\% ,$$

[3], Figure 4, with $\pm 50\%$ = scatter in dependence of the structural type and shape of bow and of the degree the forepeak is filled with water.
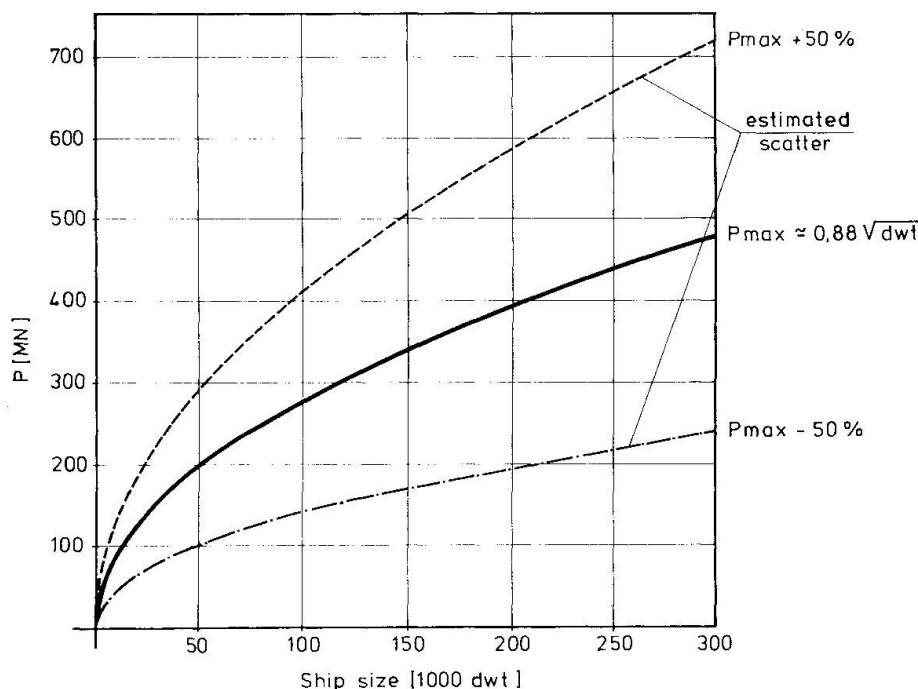

Fig.4
Woisin's approximation for the relation between the impact force P_{max} and ship's size [dwt] for bulk carriers. From [5]

3. PROTECTIVE SYSTEMS

3.1 Possibilities of Energy Conversion

The kinetic collision energy must be converted into mechanical work:

$$\Delta E = A \qquad \Delta E: \text{Collision Energy}$$

$$A = \int K \cdot d \cdot s = f_i \cdot K \cdot s \qquad A: \text{ mechanical work}$$

$$K = \frac{A}{f_i \cdot a} \qquad\qquad K: \text{ reaction force}$$

The factor f_i depends on the curve of the force deformation diagram and lies between 1 (ideal plastic, without sta-bilization), 1/2 (linear elastic), and 0 (powerless deformation), Figure 5.

For the mooring of ships the elastic range comes into consideration for energy conversion, in which no ex-change of protective devices becomes necessary. The more the probability of an impact decreases and the greater and more concentrated the forces to be absorbed become, the more important plastic deformations become which require repairs up to the point of complete replacement.
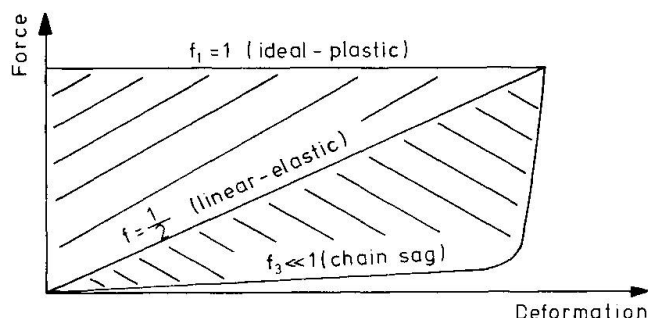

Fig.5 Possible work diagrams for con-verting collision energy

The energy to be converted in the impact may be absorbed by the protective device or an energy absorbing intermediate layer, a "fender", or by the ship itself. Generally all possibilities take place simultaneously. The reaction force thus generated has to be transmitted into the ground by the resisting structure. In order to permit an economical dimensioning of the pier and/or its protective structure, the reaction force must be limited by achieving large deformations and a factor f_i approaching 1.

3.2 Floating Systems

The floating systems are based on the idea to absorb the ship's energy advanta-geously with small forces and large deformations and to overcome considerable water depths with high-strength tension members.

The floating systems differ with respect to their type of energy conversion, to their design against being overrun, as well as to the type of their tension mem-bers and their anchorages.

3.2.1 Elastic Energy Conversion

For the temporary protection of a drilling rig in the Akashi Channel, Japan, a floating protection device was developed in 1973, which was anchored in 50m deep water [6], [7], Figures 6, 7. The device was designed for ships up to about 2000 dwt with a speed of up to 5 m/sec and collision angles of up to 15°.
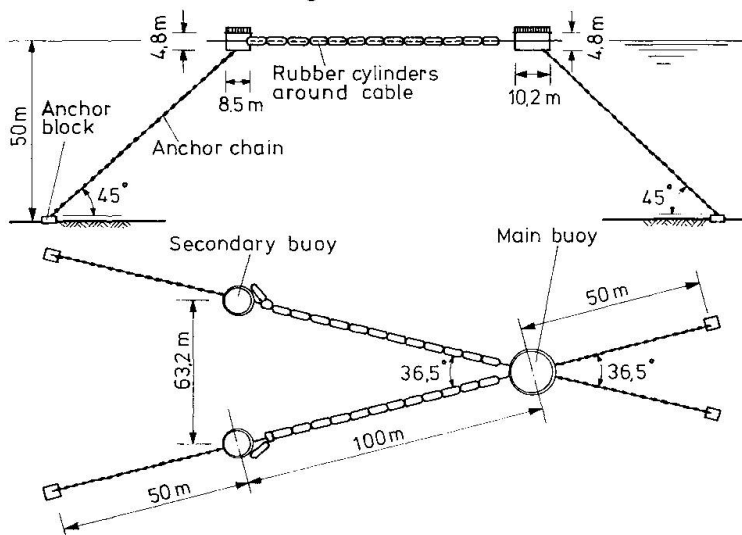

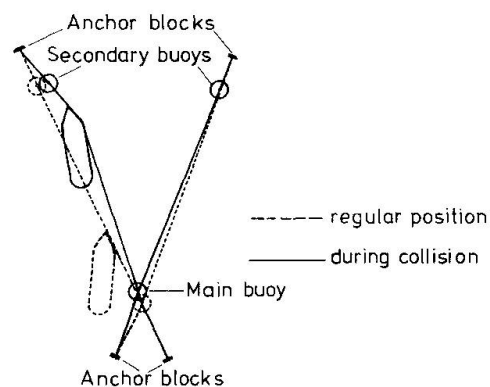Fig.6 Protective System for a drilling rig in the Akashi Channel, Japan. From [6]

Fig.7 Operation of the pro-tective system in the Akashi Channel. From [7]

After the severe collision of the S/S "Lake Illawara" with the Tasman Bridge on January 5, 1975, the future protection of the bridge was investigated /8/.

One of the protective systems developed consists of the floating interceptor system shown on Figure 8.

The device is supposed to stop a ship of 35,000 t displacement at a speed of 4 m/sec. After a forceless deformation of about 30 m the anchor cables can be stretched by roughly 35 % and each thereby creates a force of 3.5 MN. The elastic potential work capacity of two nylon cables is

Fig.8   Protective system with elastic nylon ropes. From /8/

$$A \;=\; 1/2 \cdot 300 \cdot 0.35 \cdot 2 \cdot 3.5 \;=\; 368 \text{ MNm}$$

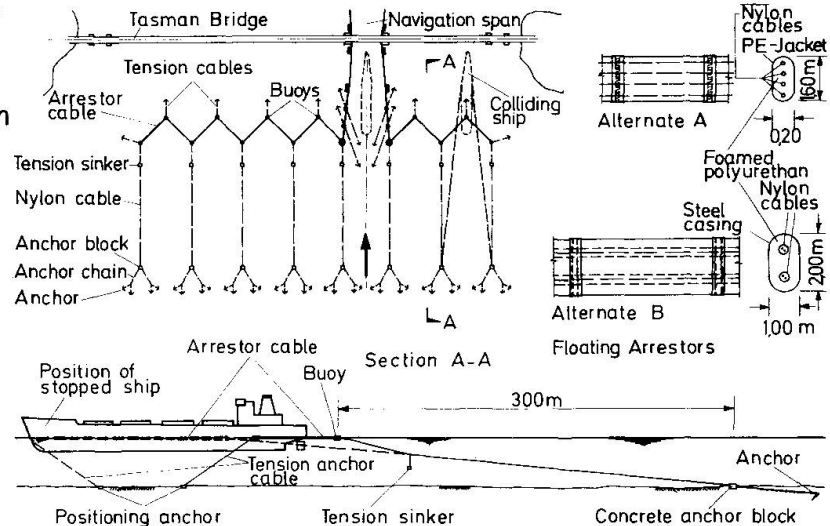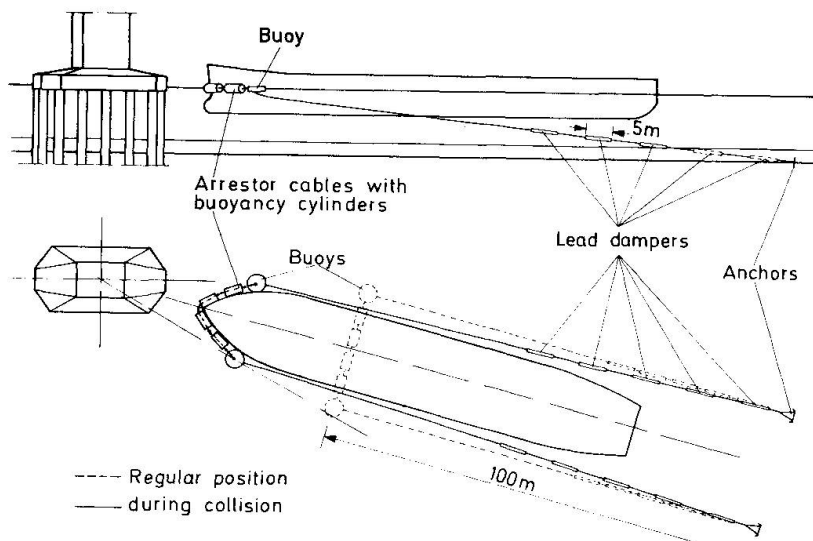$$> E_K \;=\; 1/2 \cdot 35,000 \cdot 1.05 \cdot 4^2 \;=\; 294 \text{ MNm}$$

3.2.2 Non-elastic Energy Conversion

One of the few floating systems actually realized is the one for the bridge near Taranto across the Mare Piccolo in Italy /9/. The bridge has two main openings of 152 m and a total of six piers in 12 m deep water.

The system is designed for ships of up to 15,000 t displacement with a speed of 3.1 m/s. Such a ship should be decelerated at 0.2 m/sec² over a distance of 30 m through a retaining force of 3.2 MN. The arrestor on the surface consists of chains spanning between buoys anchored to concrete foundations with chains, Fig.9.

The ship's energy is absorbed for each anchor chain by 5 dampers connected one behind the other, each 5m long. The dampers consist of a steel pipe, in which a drawbar absorbs energy through the deformation of a lead filling. The work lines of the dampers were determined by full-size model testing.

Fig. 9   Operation of the protective system for the Taranto Bridge

The braking process is characterized through (Figure 10)

$$E_K = \Delta E = 76 \text{ MNm}$$

Deceleration $b = -0.2 \text{ m/sec}^2$

Braking distance

$$s = 1/2 \cdot 3.1^2 \cdot \frac{1}{0.2} =$$

$$= 24.0 \text{ m} < 5 \cdot 5 = 25 \text{ m}$$

Medium braking force per anchor cable

$$P_A = \frac{76}{2 \cdot 24} = 1.6 \text{ MN}$$

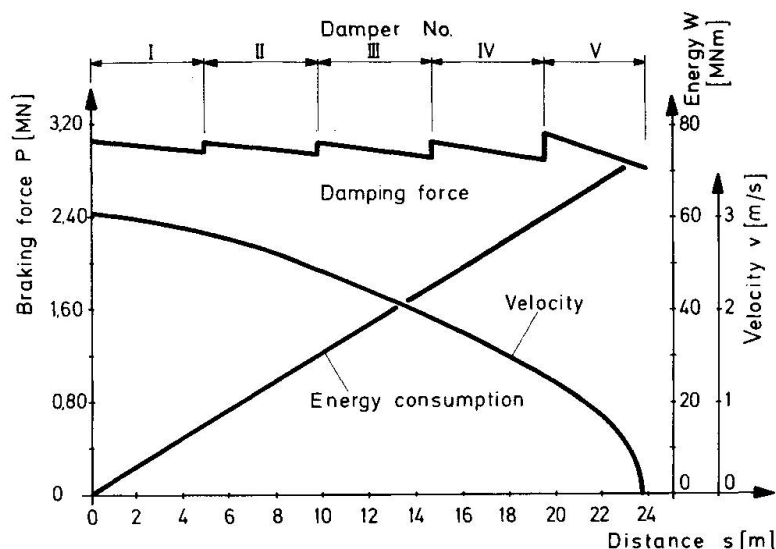Braking force on the ship

$$P_S = 3.2 \text{ MN}$$

Fig.10   Force and speed diagram of the protective system for the Taranto Bridge. From [9]

As protection against larger ships the Honshu-Shikoku Bridge Authority (Japan) has developed a so-called indirect buffer system [10], Figure 11. The colliding ship is stopped or at least slowed down considerably depending on size and speed. The energy that may still remain is supposed to be absorbed through the direct buffer system, a framework collar affixed to the pier itself, see section 3.4.

The indirect system consists of the floating intercepting device and two holding buoys. The buoys are attached to anchor blocks with vertical chains.

In a collision the floating intercepting line and the anchor chain are tightened up and the buoys submerge. As soon as the static friction of the anchor blocks is overcome, the anchors start sliding.

Fig.11   Operation of the system with sliding anchor blocks. From [10]

3.2.3 Protective Ships

In 1927, four ships were used as temporary collision protection of the main piers of the Carquinez Strait Bridge, U.S.A. [11].

It appears possible to anchor ships or pontoons of sufficient length transversely in the river in front of piers. The striking ship is completely stopped in the case of collision. The protective ship must not be severly torn up in that case, as it might otherwise sink. In order that merely the striking ship is flattened at its bow, side tanks would have to be subdivided in the protective ship and to be filled with concrete. The total kinetic energy of the striking ship has to be converted into another energy form or transferred into another energy carrier in the course of the impact.

According to Woisin, the following three energy constituents can be differentiated, Figure 12:

$$\Delta_1 E = \frac{m_2}{m_1 + m_2} \cdot E_K \qquad \text{energy absorbed practically immediately through plastic deformation}$$

$$\Delta_2 E = \frac{m_1^2}{(m_1 + m_2)^2} \cdot E_K \qquad \text{kinetic energy at first remaining in the striking ship}$$

$$\Delta_3 E = \frac{m_1 \cdot m_2}{(m_1 + m_2)^2} \cdot E_K \qquad \text{kinetic energy transferred onto the protective ship that is struck}$$

with m_1 :   striking mass including 5 % hydrodynamic additional mass

m_2 :   struck mass including 50 % hydrodynamic additional mass

E_K :   kinetic energy of the striking ship.

From these the portions $\Delta_3 E$ must be converted completely and $\Delta_2 E$ partially into other energy forms through the effect of the anchorage, e.g., into deformation work of the anchor cables (nylon cables, lead dampers), in submergence work of the protective ship, into water resistance work or into friction work of the anchors on the river bed.

In order to keep the anchor forces small, an as large as possible mass of the protective ship is necessary, see Figure 12. However, economic limitations are thereby soon be faced.
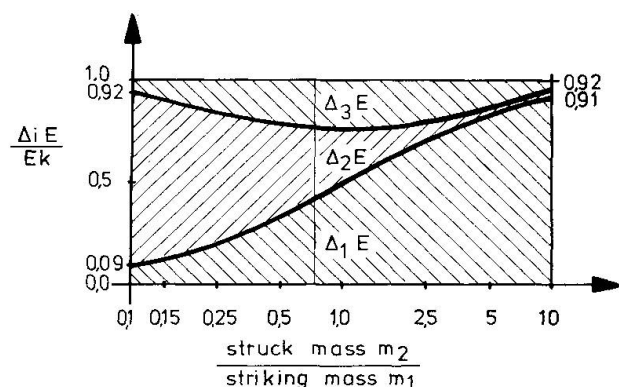
Fig.12   Distribution of the collision energy between anchored protective ship and colliding ship according to Woisin

The anchor forces reach considerable proportions; normal anchor equipment is out of question. The anchorages fore and aft have individually to be able to receive the full impact force in case of an eccentric impact.

3.2.4 Evaluation of Floating Systems

The greatest risk of the floating arrestor devices lies in the possibility that they can be submerged into the water by a ship's bow and thereby be passed over.

While the protection seems to function for the bulbous bow shapes a and b in Figure 13, this is an open question for bow shapes c and d, and depends on the buoyancy of the arrestor device, the friction between arrestor device and ship, the shape of the arrestor device — a round member will more likely roll under the bow than an oval one — and the inclination of the ship's bow. Furthermore, a ship's bow often consists of a cast iron part which may be relatively sharp-edged and can cut the anchor cables with its submerged portion.
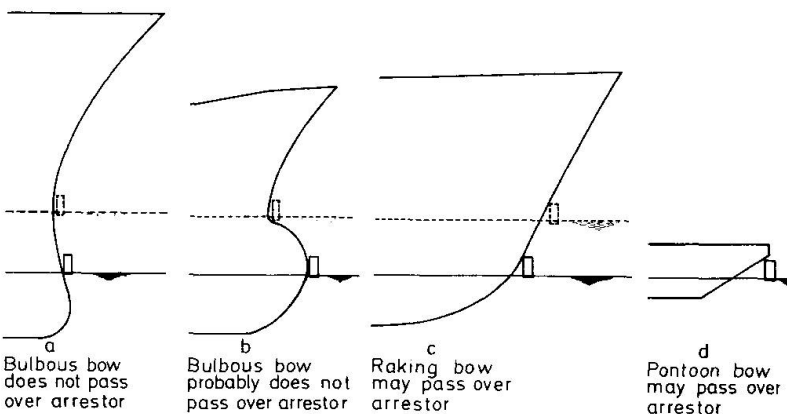
a
Bulbous bow does not pass over arrestor

b
Bulbous bow probably does not pass over arrestor

c
Raking bow may pass over arrestor

d
Pontoon bow may pass over arrestor

Fig.13   Typical bow shapes and floating systems. From /8/

Because of the possible erosion of the river, the lengths of the anchor cables of all floating protective devices may have to be adjusted frequently. Another essential disadvantage of all floating systems lies in the fact that the anchorage systems and their end linkages have to be checked continually as they are exposed to severe corrosion under water.

Chains, as was proven by Det Norske Veritas, are no reliable tension elements. On the whole, floating systems are subject to so many uncertainties that they are not considered a safe protection.

3.3 Pile Systems

Single-standing piles or pile groups of wood, steel or concrete have long been used for mooring.
In contrast to mooring operations, in which the small energy involved is received elastically by the piles, the far greater collision energy can be absorbed only through plastic deformation of the piles.

For protection of the Tasman Bridge, Australia, the two following protective systems were investigated /8/.

The one system consists of vertical prestressed concrete piles, which are fixed below in rock and above in a strong fender beam, Figure 14. The ship's energy (assumed to be 300 MNm) is absorbed at both fixings through the rotation of plastic hinges. The energy reception of a pile measuring 3 m in diameter was calculated to be 18.3 MNm for a head deflection of 5 m, yielding $A_i = 2 \cdot 8 \cdot 18.3 = 293$ MNm. Because of this significant plastic deformation the entire protective device would have to be replaced after a collision.

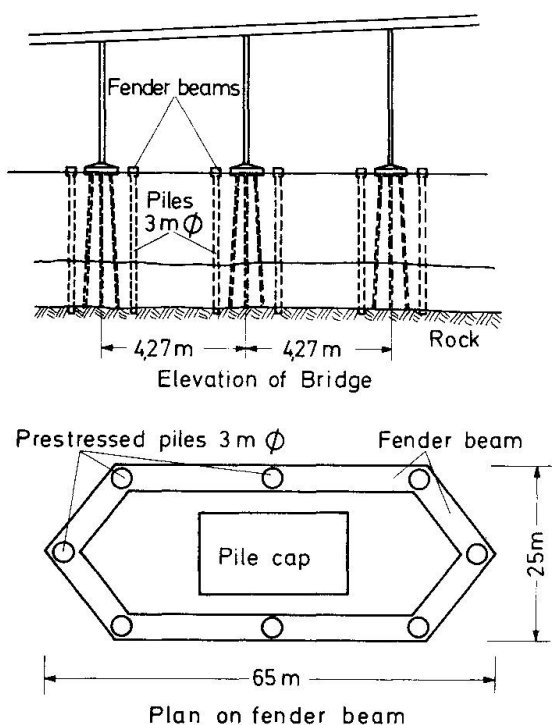Fig.14   Protective system with vertical piles. From /8/
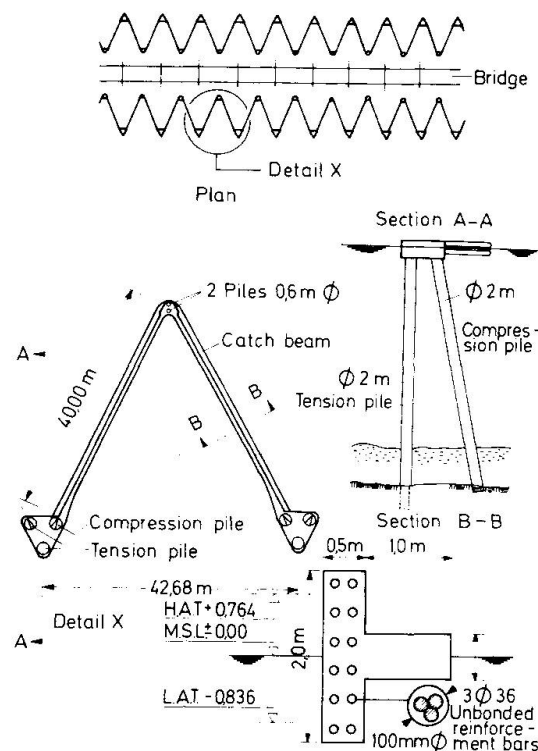
Fig.15   Protective system with tension piles. From /8/

The other system consists of V-shaped catch-beams on the surface of the water, which are anchored to tension and compression piles, Figure 15. Each of the catch-beams is reinforced with steel rods having a yield strength of 430 N/mm² and an elongation at failure of at least 22 %.

The energy of the design ship of 300 MNm is supposed to be received through plastic longitudinal deformation of the steel rods: maximum force per catch-beam

$$\text{max } P = 36 \cdot 1018 \cdot 430 \cdot 10^{-6} = 15.8 \text{ MN}$$

maximum elongation $\text{max } s = 0.22 \cdot 40 = 8.8 \text{ m}$

internal work (practically completely plastic) for two catch-beams

$$A_i = 2 \cdot 15.8 \cdot 8.8 = 278 \text{ MNm} \approx 300 \text{ MNm} .$$

The tension force of 15.8 MN is conducted into the ground by the piles elastically. The struck catch-beams have to be replaced after a collision.

3.4 Fenders

Various fender types, mostly of rubber, wood or steel were developed for the protection of ships and offshore structures in mooring operations /12/. By distributing the ship's energy through fenders the bearing pressure on the ship's hull shall not exceed 0.2 MN/m². During mooring operations the fenders remain in the elastic area.

The traditional timber fenders from beam grids can be elastically compressed by about 5 % of their thickness. Recently elastic fenders of rubber have been developed which are working in compression, shear, bending or tension. The largest of the pneumatic fenders built so far — air-filled tubes of reinforced rubber, 4.5 m in diameter and 12 m in length — can absorb an impact energy of 5.3 MNm /13/, which is considerably less than what is required in the collision of large ships.

Fenders effective in the plastic range, in which a corrugated steel pipe is compressed, achieve to date only an energy reception of 310 kNm /14/. It is practically impossible to distribute the concentrated impact forces over the necessary large number of fender units.

The framework collar for the Honshu-Shikoku Bridges, mentioned in section 3.2.2, is supposed to receive greater collision energies through successive plastic deformations of individual framework members. This development, however, appears to be in an early stage.

Great collision energies can be received in the plastic area by wood fenders; realized examples are given, e.g., in /11/. The plastic work reception capacity is indicated in /15/ for various kinds of wood. In the entire range of plastic deformation the restoring pressure remains relatively constant, in other words, the increase in force at the beginning of the impact as shown in Fig.3 does not occur.

In order to protect the fenders in smaller collisions and to keep the friction values (and thereby the energy portion to be taken by the protective system, see Fig.2) low, an outer steel plate should be provided. In impact tests on timber fenders with this steel plate the volume of the wood activated for energy consumption increased up to the double /16/, and the steel that is plastically deformed in the impact receives additional energy.

Wood fenders are relatively inexpensive and generally easily obtainable. Hardwood with appropriate pretreatment has a high longevity and is practically maintenance-free /12/.

3.5 Dolphins

3.5.1 Sliding Caissons

As the expected impact forces could not be received by the piers next to the main opening of the planned Bahrain Causeway Bridge, concrete caissons filled with sand and placed on a layer of rocks, were originally proposed for its protection /17/, Figure 16. The energy conversion is supposed to take place through the deformation of the ship's bow and by sliding of the caissons on the rock layer.
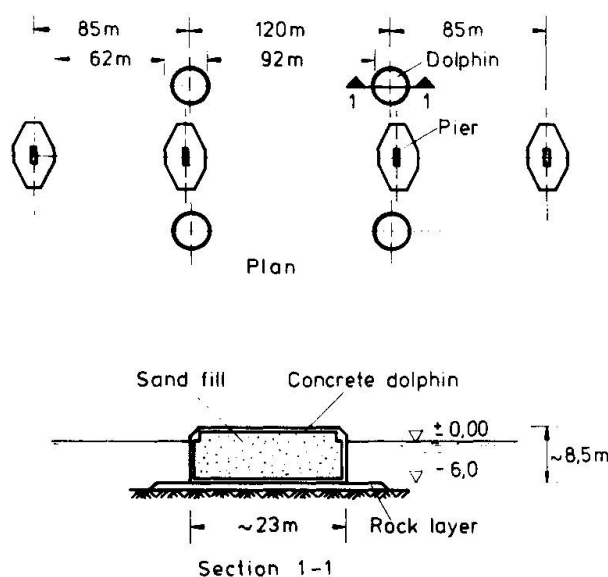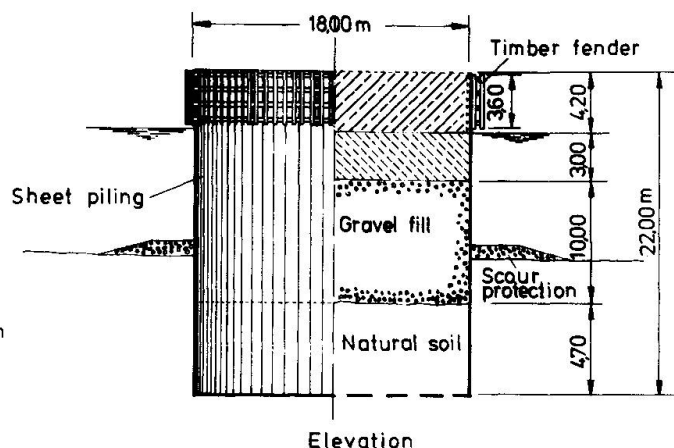
Fig. 16 Sliding caissons. From [17]

Fig.17 Circular cell

3.5.2 Fixed Dolphins

Circular cells from sheet piling, Figure 17, have already often been used as protection of bridge piers, e.g., for the Goethals Bridge and the Outerbridge Crossing, U.S.A. [18], the Rio Niteroi Bridge, Brazil [19] and the Betsy Ross Bridge, U.S.A. [20].

These cells generally consist of sheet piling filled with gravel or sand and a concrete slab on top. The fender system is mostly laid out for smaller ships. Such cells stopped a 35,000 dwt freighter with a speed of 4 m/s in the Port of Philadelphia, U.S.A. [11] and a 45,000 t tanker in front of the Outerbridge Crossing [18].

3.5.3 Caissons proposed for the Zárate-Brazo Largo Bridges

The protection proposed by the authors for the deep water piers of the two Zárate-Brazo Largo (ZBL) Bridges in Argentina, [2] and [21], consists of concrete caissons on piles with projecting, fender-protected concrete platforms, Figure 18.

The fenders of hardwood beams are 2m thick on the sides and 4m thick at the tip. They are armored on the outside with a 20 mm thick steel plating and extend 0.5 m below the low-water mark in order to prevent the penetration of driftwood and small boats. The fenders are installed on a subsidiary construction that is designed for the bearing pressure. In order to reduce maintenance the fenders are placed above water-level. In order to be effective for ships with bulbous bows, they are anchored to a platform protruding at least 3m over the foundation. If a ship with raking bow and with greater collision energy than envisioned collides, the ship is deformed in its relatively weak upper part, and smaller impact forces are generated than in the deformation of the stronger underwater part.

The platforms sits at the same height as the pile caps of the bridge piers, i.e., their lower edge is located about 2.5 m above the mid-water mark. In order to protect the piers also against flat barges at low tide, which otherwise could break off the downward projecting timber fenders and run underneath the platform onto a bridge pier, the platform edges in the end areas are extended down to the low-water mark. Due to the required width of the platform, a ship's impact may occur centrically as well as eccentrically. For the same force, the eccentric impact is the more dangerous because of the additional moment. In order to reduce the eccentric impact force, the collision angle and thereby the collision energy to be received by the protection is reduced by shaping the platform as an equal-
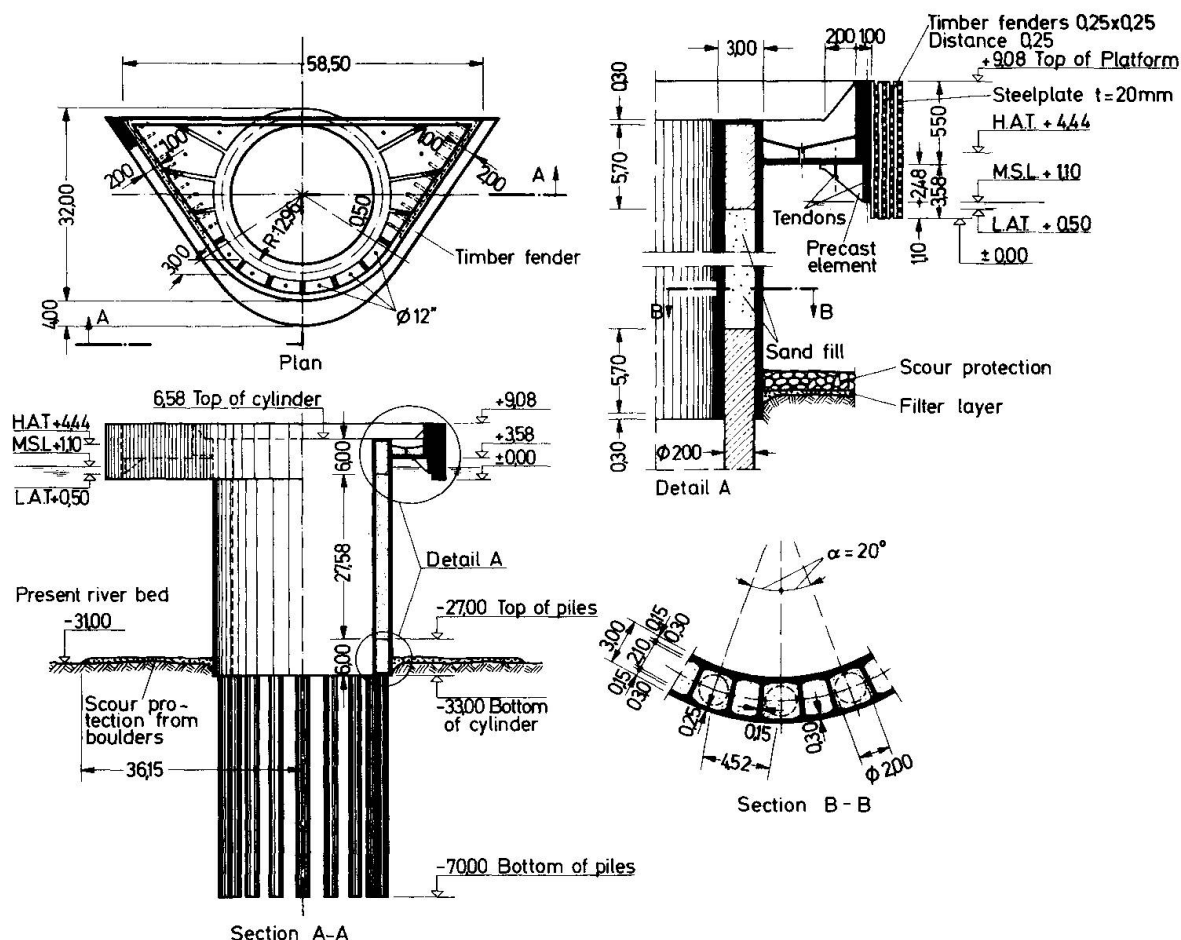
Fig.18 Dolphins proposed for the Zárate-Brazo Largo Bridges

sided triangle so that the collision energy of an eccentric impact for the given collision angles of the ZBL Bridges amounts to only about 1/3 of the ship's energy. The deformation of the fenders on the sides should not amount to more than about 1m in order to prevent that the colliding ship gets stuck in the fender and then gives more energy to the protection.

A frontal impact against the tip of the platform cannot be disregarded. The striking ship is so sluggish that during the brief impact duration of about 1-3 seconds no significant diversion from the tip of the platform takes place. The platforms are connected with caissons through their bottom slabs and radial walls which distribute the impact force over the caisson area and stiffen its upper edge.

The caissons themselves have the shape of hollow cylinders with 3m thick walls and rest on drill piles of 2m ∅ that extend all the way to the foundation elevation of the bridge piers. The circular arrangement of the piles is best suited to withstand the moments created by an eccentric impact.

The entire protective device is practically maintenance-free and is hardly subject to corrosion that would limit its efficiency.

3.5 Protective Islands

These "islands" consist of sand, gravel or boulders with a top layer of heavy stones. On soft ground it is also necessary to have a filter bed of graded gravel. The collision energy is converted through the deformation of the protective material as well as through the position shift of the ship and the surrounding water.
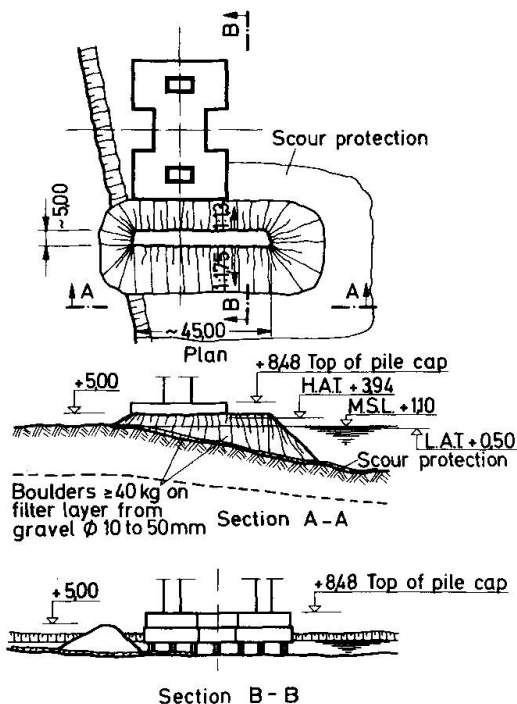
The efficiency of such islands has already been investigated in the U.S.A., in England and in France. In connection with the bridge across the Great Belt further comprehensive hydraulic model tests were conducted, the results of which were developed into a computer program [22]. The behavior of a 250,000 dwt tanker is shown in Figure 19.

The tests showed that container ships with sharp bows at collision angle $\alpha < 26°$ and tankers with cylinder bows at $\alpha < 45°$ slide off the island. The depth of penetration at greater collision angles depends, among other things, upon the ship's energy, its construction type and the island's layout.

Fig.19 Operation of protective islands from model tests. From [22]

The advantages of such islands are that they combine a high degree of safety, confirmed through model tests, with economical factors in shallow water (the fill quantity enters in the third power of the water depth). They stop a ship slowly and prevent major damages of the hull. Furthermore, they have a high longevity, are maintenance-free, and require only minor repairs through additional filling after a collision.

Their potential may be limited by the fact that the flow cross section must not be reduced so much that the water-flow speed and hence the erosion of the bed are increased excessively. That would also result in an increased danger of collision. Fillings in the form of artificial islands around the foundation of bridge piers have already frequently been used, e.g., for a pier of the Westgate Bridge, Australia, for some side piers of the abovementioned Taranto Bridge in Italy, for the Verrazano Narrows Bridge, N.Y. [5], and for the Loire bridge near St. Nazaire, France [23].

A protective island has been proposed by the authors for one pier of the Zárate-Brazo Largo Bridges which was located in shallow water, Figure 20.

Section B-B

Fig.20 Protective Island proposed for the Zárate-Brazo Largo Bridges

The width of its crown was determined on the basis of the model tests for the Great Belt Bridge.
In order to avoid a transfer of the impact force via the filling against the pile foundation of the bridge and to prevent additional loads on these piers through the weight of the filling and negative skin friction, the downstream slope ends in front of the piers.

4. SUMMARY AND CONCLUSION FOR THE PLANNING OF NEW BRIDGES

Because of the high costs of afterwards installed protective systems, considera-
tion of ship collision should be included in the concept of a bridge or offshore
structure from the very beginning.

The safest would be to found the piers on land or in very shallow water to place
them beyond reach for ships. An interesting case, although because of the great
water depth and poor bottom conditions an extreme example, are the Zárate-Brazo
Largo Bridges: the total costs of the approximately 11 km long bridge crossing
amounted to about 600 million Deutschmark, of which roughly 175 million were for
the main spans. The authors' proposed safe protection system would have cost
about 65 million Deutschmark, that is, 11 % of the total cost and 37 % of the
cost of the main spans. For this money the main spans of both cable-stayed bridges
could have been increased from 330 m to about 410 m, and thus three of the four
main piers could have been placed on dry land. A suitable scour protection would,
of course, have to be provided against possible future erosion of the riverbed.

If the water is too wide to be bridged by one span, the main span length should
at least be twice the length of the largest ship using the waterway, for naviga-
tional traffic in both directions /10/. The following possibilities are then re-
commended for the protection of the piers, the evaluation of which would depend
on the local conditions:

  - the piers and their foundations are designed in such way that the impact
    force resulting from the deformation of the ship alone can be withstood;
  - the piers and their foundations are protected by fenders which reduce the
    impact force;
  - the piers are placed out of reach for ships by means of protective islands;
  - the piers are protected by dolphins founded independently.

It must not be overlooked that not only the piers adjacent to the navigational
channel are endangered but also those away from the channel. The evaluation of
collisions according to the position of the hit piers in Table 1 shows that out
of 19 investigated accidents only 6 concerned the main spans, whereas 13 involved
the approach spans.

Bridge	Country	Year	Main pier	Side pier
Severn Railway	England	1960		X
Richmond-SanRafael	USA	1961	X	
Outerbridge	USA	1963	X	
Sorsund	Norway	1963		X
Maracaibo	Venezuela	1964		X
Chesapeake Bay	USA	1970		X
Chesapeake Bay	USA	1972		X
Sidney Lanier	USA	1972		X*
Mount Hope	USA	1975	X	
Tasman	Australia	1975		X
Fraser River	Canada	1975		X
Grand Narrows, CNR	Canada	1975	X	
Chesapeake Bay	USA	1976		X
Pass Manchac	USA	1976		X
Benj.Harrison Memor.	USA	1977		X
Union Avenue	USA	1977	X	
Burrard Inlet, CNR	Canada	1979		X*
Sunshine Skyway	USA	1980		X
Newport Bridge	USA	1981	X	
			19	6	13

* superstructure of side span hit

Table 1: Ship - bridge collision listed after their location to the main span

Following the serious accident with the Tasman Bridge an investigation was undertaken to consider the feasibility of providing protection of all twenty piers in jeopardy /8/. However, the fixed protection systems that were considered safe proved to be so expensive that it was decided to build the Second Hobart Bridge close by and to leave the Tasman Bridge without protection. The volume of traffic alone would not have justified building a second bridge; however, it is to serve as a standby if the Tasman Bridge would be hit again /24/. Massive concrete caissons up to 45 m high and 25 m in diameter were selected for the foundations of the Second Hobart Bridge to enable it to withstand impacts of 10,000 t ships.

REFERENCES

1. LLOYD'S Register of Shipping, Statistical Tables 1980. London 1980.

2. SAUL R. and SVENSSON H., Zum Schutz von Brückenpfeilern gegen Schiffsanprall (On the Protection of Bridge Piers against Ship Collision). Die Bautechnik 58(1981), p.326-335, 374-388.

3. SAUL R. and SVENSSON H., On the Theory of Ship Collision against Bridge Piers. IABSE Proceedings P-51/82, p.29-38.

4. WOISIN G. and GERLACH W., Beurteilung der Kräfte aus Schiffsstößen auf Leuchttürme in See (Valuation of Forces due to Ship Collision on Off-shore Lighthouses). German Technical Reports for the Eighth International Seamark Conference, Stockholm 1970.

5. FRANDSEN A.G. and LANGSO H., Ship Collision Problems:I. Great Belt Bridge,II. International Enquiry. Publications IABSE, 1980, p.81-108.

6. YOKOHAMA RUBBER CO., LTD., Yokohama Protection Floats Employed for Bridge Pillars. News Release, Tokyo, April 1973.

7. ODA K. and NAGAI S., Protection of Maritime Structures against Ship Collisions. Proc. 15th Coastal Engineering Conference, ASCE. Honolulu, July 1976, p. 2810-2829.

8. MAUNSELL and PARTNERS with BRADY P.J.E., Second Hobart Bridge, Report on Tasman Bridge — Risk of Ship Collision and Methods of Protection. September 1978.

9. Brochure of Società Applicacioni e Progrettaccioni Speciali, SpA (S.A.P.S.), Rome, undated.

10. HONSHU-SHIKOKU BRIDGE AUTHORITY, Study Report on the Navigational Safety of the Honshu-Shikoku Bridges. Tokyo 1973.

11. OSTENFELD Ch., Ship Collisions against Bridge Piers. Publications IABSE,1965, p. 233-277.

12. RINNE H.G., Fenderungen im Hafenbau (Fenders in Harbour Construction). Ph.D. thesis TH Hannover, 1962. Jahrbuch der Hafentechnischen Gesellschaft, Vol. 25/26(1958/61). Berlin, Göttingen, Heidelberg: Springer 1962.

13. Brochure of Yokohama Rubber Co., Ltd., Pneumatic Rubber Fenders. Catalog No. NASOBE, Tokyo 1978.

14. Brochure of Andre Rubber Co., Ltd., Plastic Energy Absorption Corrugated Unit (P.E.A.C.U.). Surbiton 1971.

15. U.S. DEPARTMENT of AGRICULTURE, Wood Handbook. Forest Service, Agriculture Handbook No.72. U.S. Government Printing Office, August 1972.

16. GIBBS and COX, INC., Criteria for Guidance in the Design of Nuclear Powered Merchant Ships. U.S. Department of Commerce, 1960.

17. SAUDI-DANISH CONSULTANTS, Saudi Arabia - Bahrain Causeway, Design Memorandum No.4, Review of Ship Impact on Bridge Piers. Riyadh, Copenhagen, August 1978.

18. HAHN D.M. and RAMA H.E., Cofferdams protecting New York Bridges from Ship Collisions. Civil Engineering - ASCE, February 1982, p.67-68.

19. WEINHOLD H., Die Gründung der Brücke über die Guanabara Bucht in Rio de Ja- neiro (The foundation of the Bridge over the Guanabara Bay in Rio de Janeiro). Der Bauingenieur 48(1973), Vol.1, p.1-13.

20. Dolphins Protect Piers of 2.5 km Long Bridge. World Construction, December 1975, p.75.

21. LEONHARDT F., ZELLNER W. and SAUL R., Zwei Schrägkabelbrücken für Eisenbahn und Straßenverkehr über den Rio Paraná (Argentinien) (Two Cable-stayed Bridges for Road and Railway Traffic across the Rio Paraná, Argentina). Der Stahlbau 48(1979), p. 225-236, 272-277.

22. NIELSEN A.H. et al., Rubble Mound Slopes as Protection against Ship Impact. Danish Hydraulic Institute, Copenhagen 1979.

23. SCHLEUCH G., Brückenschlag über die Mündung der Loire (Bridge across the Loire- mouth). VDI-Nachrichten Nr.38, Sept.19, 1975, p.4-5.

24. FERGUSON H., Standby for High Risk Tasman Bridge. New Civil Engineer, Aug.30, 1979, p.9.

Almö-Bridge over the Askeröfjord, Sweden
Hit on January 18, 1980, by a 15.000 t - freighter. 8 persons killed.
Photo: Courtesy of Construction News, London, England

Leere Seite

Blank page

Page vide